

# Piezoelectric Polymeric Foams as Flexible Energy Harvesters: A Review

Manauwar Ali Ansari\* and Patcharapon Somdee

Piezoelectric energy harvesters (PEHs) have the potential to power low-power electronic devices and can advance, self-powered, autonomous electronics to the next level. Conventional ceramic-based piezoelectrics have various properties such as fragility, rigidity, toxicity, high density, and lack of design flexibility which limit their use in more flexible environments. A ton of research has been carried out and published on novel piezomaterials, their transduction mechanisms, analytical models, and electrical circuits to improve various aspects of PEHs. Among these materials, studies on polymeric cellular (or foamed) ferroelectrets or piezoelectrets as PEHs have grown significantly since their discovery. Also, very limited or short reviews are available covering only few aspects. There is a necessity of recognizing their past and present advances in their various generation technology and polymer systems. Herein, a broader review of almost all conventional and recent polymeric foam-based piezoelectrics for PEH applications is summarized. These cellular polymer piezoelectric systems either in bulk, composite, layered, or film form can be fabricated, and depending on the application and conditions, different polymers groups, mainly, polyolefins, polyester, fluoropolymer, and others, are considered. Their applications and future perspectives are also presented and discussed.

which resulted in comparatively high energy output than other piezoelectrics.<sup>[3]</sup> Although PZT is a common material, its properties such as fragility, rigidity, toxicity, high density, and lack of design flexibility have limits on its use. Therefore, highly compatible piezoelectrics from material class polymers and ceramic-fiber composites could be mainly considered. Until now, the most popular polymer-based piezoelectrics reported is polyvinylidene fluoride (PVDF), having more flexibility and a comparatively low piezoelectric coefficient. Researchers have also undertaken various efforts to enhance the piezoresponse of PVDF and their approaches based on either fabrication methodology or increasing the  $\beta$ -phase percentage in the composition.<sup>[4,5]</sup> Besides PZT and PVDF, now, a lot of their material systems come in the form of piezoelectric single crystals,<sup>[3]</sup> nanostructured ceramics,<sup>[6,7]</sup> ceramic-polymer composites, nanoparticles-polymer composite foams,<sup>[1,8]</sup> molecular monolayers,<sup>[9]</sup> molecularly doped polymeric foams,<sup>[10]</sup> space-charge electrets,<sup>[11]</sup> etc.

## 1. Introduction


Today, piezoelectric materials have increasingly become popular due to their various engineering applications such as sensors, actuators, and energy harvesters (EHs).<sup>[1,2]</sup> So far, lead zirconate titanate (PZT) has been the most popular ceramic-type piezoelectric that has been investigated due to its large coupling coefficient ( $d_{33}$ )

Recently, scientists have started studying the polymeric cellular (foam) piezoelectrets for PEH applications.<sup>[12]</sup> The polymeric foam piezoelectrets (or ferroelectrets) were first discovered in Finland in the 1980s.<sup>[13]</sup> This type of piezomaterial is a dielectric having permanent electric charge similar to permanent magnets having permanent magnetic fields. These are called ferroelectrets showing piezoelectric-like properties, opposite to conventional piezoelectric materials. Piezoelectricity is induced in these materials by a polarization process that imparts charge which is permanently trapped in foam voids by applying either electrical or mechanical stimuli that make the charged voids macroscopic dipoles. Piezoelectric foams have advantage over conventional piezopolymeric materials due their large piezoelectric coefficient ( $d_{33} = 250 \text{ pC N}^{-1}$ ), which is almost seven times higher compared with PVDF ( $d_{33} = -33 \text{ pC N}^{-1}$ ). The foams void-cell-like structure also gives them a low weight and great compliance. Moreover, piezoelectric systems made from cellular polymers either in films or bulk forms have special interests because of their low material cost, ease of processing, the possibility to make flexible thin films, low density, etc.<sup>[14]</sup>

There have been many reviews reported so far. Mohebbi et al.<sup>[15]</sup> presented a review based on ferroelectret materials, their processing, and applications and also discussed the various parameters affecting  $d_{33}$  coefficient such as pressure, gas breakdown strength, fillers, and working temperature. Sappati et al.<sup>[16]</sup>

M. A. Ansari  
Hevesy György PhD School of Chemistry  
Eötvös Loránd University  
Pázmány Péter sétány 1/A, H-1117 Budapest, Hungary  
E-mail: ansarima@student.elte.hu

P. Somdee  
Department of Materials Engineering  
Rajamangala University of Technology Isan  
744 Suranarai Road, Muang-Nakhon Ratchasima 34000, Thailand

 The ORCID identification number(s) for the author(s) of this article can be found under <https://doi.org/10.1002/aesr.202200063>.

© 2022 The Authors. Advanced Energy and Sustainability Research published by Wiley-VCH GmbH. This is an open access article under the terms of the Creative Commons Attribution License, which permits use, distribution and reproduction in any medium, provided the original work is properly cited.

DOI: 10.1002/aesr.202200063

reviewed different piezoelectric papers and polymers, Kaczmarek et al.<sup>[8]</sup> reviewed various classes of piezoelectric polymers. Zhang et al.<sup>[17]</sup> discussed ferroelectrets' materials, manufacturing technique, and modeling. Safaei et al.<sup>[2]</sup> comprehensively reviewed piezoelectric energy harvesters (PEHs) based on various types of materials and methods covering the research published between 2008 and 2018. Mishra et al.<sup>[1]</sup> explored polymers and nanocomposite-based piezoelectrics in PEH applications. Surmenev et al.<sup>[18,19]</sup> summarized the recent accomplishments in the advancements of novel hybrid lead-free PVDF or PVDFTrFE-based piezoelectrics and pyroelectrics for biomedical applications. However, currently, there are very limited or no reviews available to broadly and separately cover the polymer foam (or cellular)-based piezoelectrets considering recent advances in their generation method and various polymer material groups.

Therefore, the aim of this article is to summarize the current advancements in piezoelectric cellular polymers, based on conventional and recently developed generation techniques in view of various polymer classes. In this review, Section 2 provides the general definition and the principle of piezoelectricity and PEHs. Section 3 gives the division of polymeric piezoelectric foams based on their classical and recent variants such as space-charge piezoelectrets (single and stacked), cellular piezoelectric composites, molecularly doped piezofoams, and solid-electrolyte-filled piezoelectrets. Further, each type of piezofoam is reviewed in view of various polymers groups such as polyolefins (PP, IXPP, PE), polyesters (PET, PEN), fluoropolymers (PTFE, FEP, AF), and others (COP & COC, PC, PDMS, PVDF, PLA, and PU) from the past available literature. Section 4 and 5 provide a discussion on their application as PEHs and their future scope, respectively. Finally, the main conclusions are given in Section 6.

## 2. Piezoelectricity: Theory and Principle for Energy-Harvesting Devices

The ability of certain materials to convert from mechanical (shock, vibration, etc.) energy to electrical energy without any external energy input, or vice versa, is called piezoelectricity, and the materials having this property are known as piezoelectric materials or simply "piezoelectrics". The process of converting energy from mechanical to electric is called direct piezoelectric

effect and the reverse process is referred to as the converse piezoelectric effect, as depicted in **Figure 1a,b**. Almost all the sensors and transducer systems are associated with direct effect, whereas, actuators are based on converse effect. The direct relation between the polarization density and the stress of the materials (bulk) is responsible for the reversible process.<sup>[17]</sup> This property can be calculated via a piezoelectric  $d_{33}$  coefficient with the unit of  $\text{pC N}^{-1}$ .

This piezoelectric phenomenon is mainly attributed to certain types of crystal lattices having elemental structures. The total charge (positive and negative) balance equilibrium within these crystal structures stays neutral across the polar axis (virtual). This equilibrium is unbalanced or gets disturbed whenever mechanically strained or vibrated, allowing the dipoles to become irregular and producing an electrical charge.<sup>[2]</sup> Imposing physical stress either compression or tension results in charge balance disruption, also deforming the internal crystal structure. The charges (positive and negative) are then separated by the destruction of the molecule's neutrality, generating surface charge density for the electrodes to be collected.<sup>[21]</sup>

The materials having no polarization and no piezoelectric effect can be made piezoelectric by an operation called poling, in which generally, a strong electric field is applied close to their Curie temperature. This process generates polarization by enabling the movement of the free molecule and aligning the dipoles in a singular orientation along the direction of the applied electric field. When the temperature is lowered to normal room temperature and the electric field is taken away, the dipoles retain their closely aligned polarization in a continuously locked configuration, displaying piezoelectric behavior. Polycrystalline materials, however, have the ability to adjust polarization if necessary, and by changing the poling conditions, their polarization degree can also be adjusted easily by varying the poling conditions.<sup>[22,23]</sup>

The direct as well as converse piezoelectric process can be well represented by the two equations as follows.<sup>[24]</sup>

Direct piezoelectric effect

$$D_i = e_{ij}^{\sigma} E_j + d_{im}^d \sigma_m \quad (1)$$

Converse piezoelectric effect

$$\epsilon_k = d_{jk}^c E_j + S_{km}^E \sigma_m \quad (2)$$

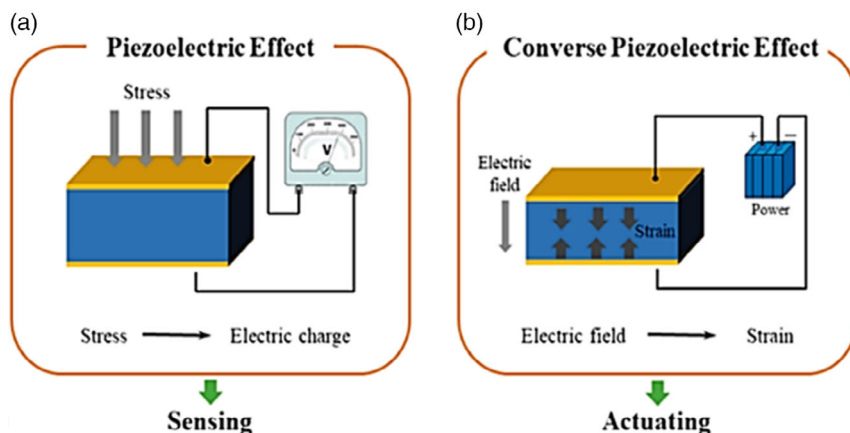


**Figure 1.** a) Direct and b) converse piezoelectric effect. Reproduced with permission.<sup>[20]</sup> Copyright 2018, Springer Nature.

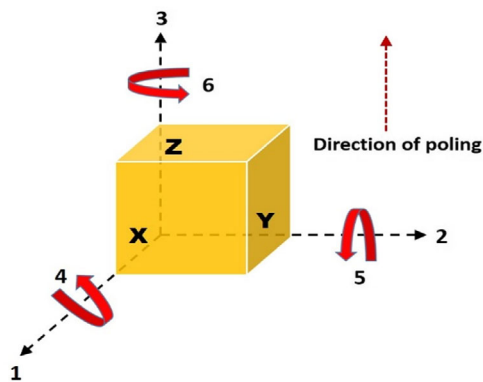


**Figure 2.** Three co-ordinate axes direction systems in piezoelectric materials. Reproduced with permission.<sup>[1]</sup> Copyright 2018, Wiley-VCH GmbH.

where  $D_i$  is the dielectric displacement,  $E_i$ , the electric field vector,  $\epsilon_k$  is the mechanical strain vector,  $\sigma_m$  is the mechanical stress vector,  $d_{im}^d$  and  $d_{jk}^c$  are piezoelectric coefficients,  $\epsilon_{ij}^\sigma$  is the dielectric permittivity; and  $S_{km}^E$  is the elastic compliance matrix. By considering the fact that the process of direct mainly associated energy-harvesting systems and devices and the converse process is with actuators, the significance of subscripts and superscripts used in Equation (1) and (2) is given in more detail. The superscripts  $d$  and  $c$  symbolically denote the direct and converse piezoelectric equations, respectively. The subscripts

$i$ ,  $j$ , and  $k$  denote the directions of the coordinate system inside the material. The superscripts  $\sigma$  and  $E$  represent the dielectric constant measurement under constant mechanical stress and constant electric field, respectively.

The axes denoted as 1, 2, 3, as shown in **Figure 2**, are similar to the Cartesian coordinate axes  $x$ ,  $y$ ,  $z$  which are used to define the three direction indices  $i$ ,  $j$ ,  $k$  in piezoelectrics. The polarization direction is defined by  $z$ -axis or direction 3. The shear motion or rotational motion is specified by the subscript  $m$  around the axes 1, 2, and 3 and is denoted here as 4, 5, and 6, respectively. The mode of operation can also be determined via these indices, wherein the electric field direction corresponds to the imposed mechanical stress/strain of a PEH.<sup>[25,26]</sup>

### 3. Types of Polymeric Piezoelectric Foams

There are a broad range of cellular or foamed polymer piezoelectrets available in the literature. They can be divided into five main groups such as conventional space-charge piezoelectrets, layered or stacked piezoelectrets, cellular piezoelectric composites, molecularly doped piezoelectric foams, and solid-electrolyte-filled piezoelectric (**Figure 3**). This classification is based on conventional and recently developed techniques to advance their piezoelectric properties.

The conventional space (or voided)-charge polymers or ferroelectrets, or piezoelectrets, are cellular-polymer films, made via the plasma discharge of the internal void gas, and their piezoelectricity

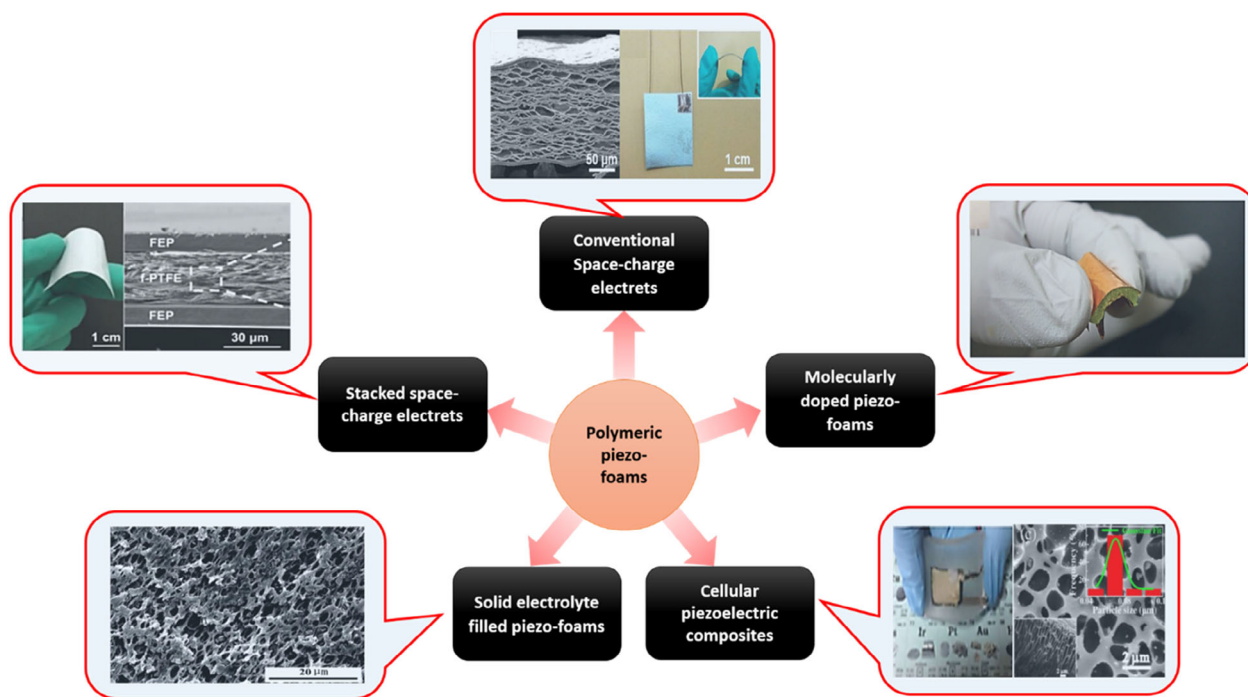


**Figure 3.** Different types of piezoelectric foams based on conventional and recently developed techniques. Conventional space-charge electrets. Reproduced with permission.<sup>[27]</sup> Copyright 2015, Wiley-VCH GmbH. Stacked space-charge electrets. Reproduced with permission.<sup>[28]</sup> Copyright 2016, Wiley-VCH GmbH. Solid electrolyte filled. Reproduced with permission.<sup>[29]</sup> Copyright 2017, The Royal Society of Chemistry. Cellular piezoelectric composites. Reproduced with permission.<sup>[30]</sup> Copyright 2016, AIP Publishing. Molecularly doped piezofoams. Reproduced with permission.<sup>[10]</sup> Copyright 2016, The Royal Society of Chemistry.

is generated through dimensional alteration of artificial macroscopic dipoles. Multilayer piezoelectrets can be used to enhance the generated voltage or current and hence the total power output depending on whether the layers have a series connection or a parallel connection. Polymeric cellular composites have many specific properties such as low specific weight, strong temperature resistance, and a higher piezoelectric constant ( $d_{33}$ ), making them the most important materials in modern electronic applications. The molecularly doped piezofoams are new types of piezoelectric materials in which electric polarization is not generated due to the foam structure, unlike in conventional space-charge electrets, but simply responsible for desirable mechanical properties, and the highly polar foreign (dopant) molecules are responsible for piezoelectricity phenomenon.<sup>[10]</sup> Piezoelectricity in the novel solid polyelectrolyte-filled cellular polymer is attributed to the strong action of intrinsic polarity and orientation of molecular dipoles of polymer (e.g., PVDF) cells, formed when pressure crystallized, with artificial macroscopic solid-electrolyte (e.g., Nafion) dipole fillers on several micrometer scale, generated via their internal ionic mobility during the deformation of the cell wall.<sup>[29]</sup>

### 3.1. Space-Charge Piezoelectrets (Single and Stacked)

Cellular polymeric films can be generated either in a closed mold<sup>[31]</sup> or by thermoforming<sup>[32]</sup> using many different processes. In general, voided (space) charge electrets or cellular polymeric film can be fabricated via two common methods: 1) stretching or 2) foaming (Figure 4). The stretching method involves the fabrication of a polymer composite film (particles filled) and stretching it to initiate cells (voids) around the filler particles through decohesion/delamination at the particles interface. The foaming

method comprises creation of cells via gas introduction just like in a normal foaming process.<sup>[15]</sup> Piezoelectricity can be generated in the cellular structures by introducing gas (e.g., Air, Ar, N<sub>2</sub>, N<sub>2</sub>O, etc.) into the cells and its ionization with an external high-voltage electric field. This may be created with the use of devices like corona discharge.<sup>[33]</sup> The schematic procedure is presented in the right part of Figure 4. The inner Paschen breakdown, which is initiated whenever charging voltage exceeds the gas breakdown threshold voltage, is responsible for charge deposition in cells. A sequence of dielectric barrier discharges (DBDs) is used to charge the interior cell surfaces in this approach.<sup>[34,35]</sup> As a result, macroscopic dipoles are created due to the separation and trapping of opposite charges on the interior upper and lower surfaces of the cells through the DBD process.

An effective method for enhancing mechanical-to-electrical energy conversion using piezoelectrets could be folding and stacking the films and hence increasing the layer numbers. Increasing the number of layers subjected to mechanical force is a good idea. The increased cellular electrets layered structures generally provide enhanced surface charge density and therefore the electromechanical properties of the piezoelectrics system. Pondrom et al.<sup>[36]</sup> presented stacks of 9 and 10-layer piezoelectrets. The harvesters generated power of  $1.3 \mu\text{Wg}^{-2}$  when periodically excited with 140 Hz compression. The output power for the system of a single layer was enhanced to 5 mW at a frequency of 700 Hz. In 2015, Ray and Anton<sup>[37]</sup> made a system with a 20-layered stack to enhance the performance, which was previously proposed by Pondrom et al.<sup>[36]</sup> The stack was excited periodically with compression and connected to charge a capacitor. The output was found around  $3.8 \text{mWg}^{-2}$  with 650 k $\Omega$  optimal load resistance. Also, his stack was configured for charging a 1 mF capacitor with the potential 1.2 V within 45 min, while

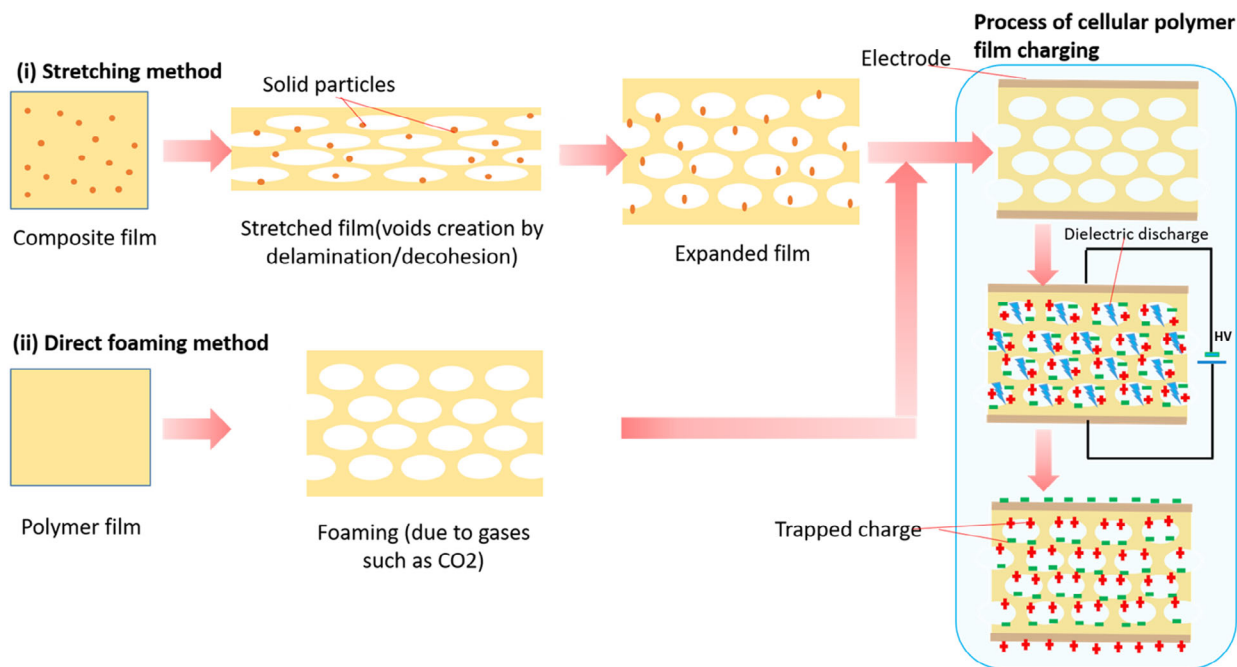


**Figure 4.** Method of generation for stacked space-charge electrets: i) stretching method and ii) direct foaming method. Reproduced with permission.<sup>[33]</sup> Copyright 2010, SPIE.

being imparted with harmonic compression at 124.4 Hz and 0.5 g acceleration. An average value of  $d_{33}$  was found as  $704 \text{ pC N}^{-1}$  for the 20-layer stack at all frequencies, which were equivalent to  $\approx 35 \text{ pC CN}^{-1}$  for each layer.

### 3.1.1. Polyolefin-Based Piezoelectric Foams

**Polypropylene (PP)-Based Piezoelectrets:** Polypropylene (PP)-based wearables and self-powered electronics replaced the serious issues of batteries and can give a comfortable and sustainable interactive service for humans. Paajanen et al.<sup>[38]</sup> reported a strong electromechanical effect, that is,  $d_{33}$  coefficient of PP-based ferroelectrics via corona charging at 100–450 Wa or at 100–140 Wa in ambient nitrogen or in nitrous oxide, respectively, with corona voltages of up to 60 kV. A maximum  $d_{33}$  coefficient of  $790 \text{ pC N}^{-1}$  was obtained when the air within cells was replaced with  $\text{N}_2$  via successive low and highpressure treatment at temperatures 293 or 313°K. Hillenbrand et al.<sup>[39]</sup> investigated piezoelectricity in cellular PP with thickness consisting of 50–100  $\mu\text{m}$  in the structure of bilayers or multilayers composed in the solid or voided form including an extra air layer. The quasistatic coefficients of the cellular PP were of the order of 100–350  $\text{pC N}^{-1}$ . The  $d_{33}$  of bilayer or multilayer structured samples was significantly larger, reaching up to 20 000  $\text{pC N}^{-1}$  in some cases. Also, a decrease toward larger frequencies was noted for the single-layer sample.

Wegener et al.<sup>[40]</sup> investigated the  $d_{33}$  coefficient for cellular structured PP films through controlling the cells' inflation pressure. An inverse trend was found among the elastic modulus and  $d_{33}$  coefficient. A  $d_{33}$  of  $306 \text{ pC N}^{-1}$  for the softest cellular PP film was achieved by inflation at 2 MPa, which was 2 times an improvement over the previous result.<sup>[41]</sup>

Qiu et al.<sup>[42]</sup> studied the piezoproperties of a preinflated PP in two ionizing gas conditions; first, the sample with  $\text{SF}_6$  as the ionizing gas was charged under a pressure of 400 kPa via the corona method at a voltage of  $-60 \text{ kV}$  for a charging time of 15 s, and second, the same sample but air as the ionizing gas was charged at atmospheric pressure via the same method at a voltage of  $-32 \text{ kV}$  for 15 s. They reported a large enhancement in  $d_{33}$  of  $350 \text{ pC N}^{-1}$  for PP films saturated with  $\text{SF}_6$  as compared with  $d_{33}$  of  $\approx 215 \text{ pC N}^{-1}$  for the samples with air media. However, the reported  $d_{33}$  of the cellular-structured PP films with  $\text{SF}_6$  saturation was far lower than that with  $\text{N}_2$  saturation, that is,  $790 \text{ pC N}^{-1}$ .<sup>[38]</sup>

Sborikas and Wegener<sup>[43]</sup> also reported the same inverse trends among elastic modulus and  $d_{33}$  coefficient of cellular PP piezoelectrets, as reported by Wegener et al.<sup>[40]</sup> They demonstrated a high piezoelectric coefficient up to  $130 \text{ pC N}^{-1}$  for a mechanically soft cellular structure obtained by film expansion and electric charging. Hence, the resonance frequencies were decreased down to  $\approx 233 \text{ kHz}$  because of increment in film thicknesses.

Anton et al.<sup>[44]</sup> reported PP foam-based vibration energy harvesting (VEH). They used commercial Emfit, Corp.-made foam and fabricated a pretensioned EH of dimensions  $15.24 \text{ cm} \times 15.24 \text{ cm} \times 85 \mu\text{m}$ . When energized longitudinally (31 mode) at 60 Hz excitation with a displacement of  $\pm 73 \mu\text{m}$  (p–p), that is, producing an acceleration of value  $\pm 10.38 \text{ g}$ , 8 V peak is generated through this system. A constant  $d_{33}$  coefficient of  $\approx 175 \text{ pC N}^{-1}$  was found at frequencies 10 Hz–1 kHz. Also, when connected to a capacitor of 1 mF, the system could take 30 min to charge the capacitor up to 4.67 V while generating the average power of about  $6.0 \mu\text{W}$ . This value of output power was comparable with polymer piezoelectrics and conventional piezoceramics.

Wu et al.<sup>[27]</sup> produced a flexible generator made of cellular PP with the highest peak power density of  $\approx 52.8 \text{ mWm}^{-2}$  for EHs and health-monitoring uses (Figure 5a,b). The measured  $d_{33}$  coefficient was  $\approx 19 \text{ pC N}^{-1}$  for the multilayered PP film and this value increased to  $\approx 205 \text{ pC N}^{-1}$  in case of the expanded cellular PP. Also, this value was found to be stable for many weeks at 60 °C. Luo et al.<sup>[45]</sup> investigated the PP foams-based piezoelectret with single-layer and multilayer stacking for the application of EH and sensors worn by the human body. This was based on a person's footfall, implemented by an electrodynamic system, applied compressive pressure, and momentum compared with power output using an electrodynamic device. Peak strength, output pulse length, and strike energy were extracted experimentally. In addition, a condenser was charged by a corrective device for the energy output of single-layer and multilayer piezoelectrets. A ten-layer ferroelectrometer had 29.1 times the charging potential with the piezoelectret of one layer. The authors also displayed its ability to energy generation and control a standard low power consumption sensor.

Recently, Mohebbi et al.<sup>[46]</sup> fabricated another PP foam-based piezoelectret material using  $\text{N}_2$  as the ionizing gas and measured a high  $d_{33}$  coefficient of  $550 \text{ pC N}^{-1}$ , that was two times higher

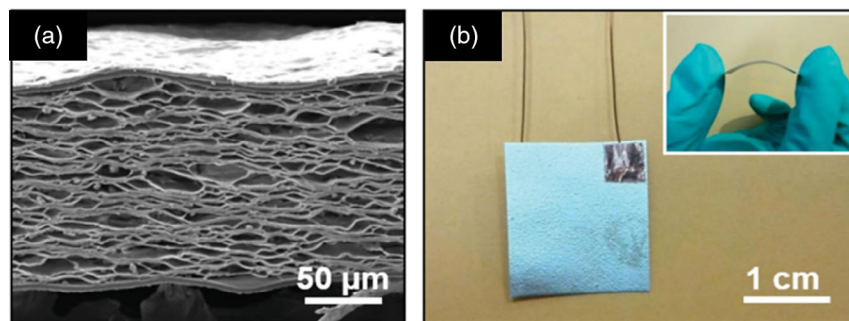


**Figure 5.** a) Scanning electron microscopy (SEM) image of the cross section of the cellular PP after expansion. b) Digital photo of a CPPFG and the inset shows its flexibility. Reproduced with permission.<sup>[27]</sup> Copyright 2015, Wiley-VCH GmbH.

than the coefficients by previously reported literatures for fabricated foams using air as the ionizing gas. Again in 2017, the same group<sup>[47]</sup> studied the effect of temperature, pressure, and time (postprocessing parameters) on PP-foam piezoelectrets. They reported the  $d_{33}$  coefficients 800 and 550 pC N<sup>-1</sup> for treated and untreated samples, respectively. In 2018, Mohebbi and Rodrigue<sup>[48]</sup> optimized a cellular PP film with AR of 6.6 using N<sub>2</sub> (ionizing medium) and measured  $d_{33}$  of  $\approx 800$  pC N<sup>-1</sup>. The electrode charge density was  $\approx 2.10$  mC m<sup>-2</sup>, capacitance  $\approx 465$  pF, and higher stored energy  $\approx 1,824$  pJ. When air was replaced with N<sub>2</sub>, they noted a significant improvement of 20% and 80% in the capacitance as well as stored energy of the samples, respectively.

More recently, Samadi et al.<sup>[49]</sup> fabricated a piezo-PP foam through the injection molding operation to be used in a possible cost-effective bone texture scaffold. The test of biocompatibility shows increased cell biocompatibility by foaming. They reported that a unique peak-to-peak potential for a 2 mm-thick foam sample was 84.02 mV N<sup>-1</sup>, which was 10 times higher than the 3 mm-thick sample.

**Irradiation-Crosslinked PP (IXPP)-Based Piezoelectrets:** In 2009, Zhang et al.<sup>[50]</sup> reported hot-pressed-treated and corona-charged cellular piezoelectret films based on cellular irradiation cross-linked PP (IXPP) and obtained quasistatic piezoelectric  $d_{33}$  coefficients up to 400 pC N<sup>-1</sup> for room temperature-charged samples. They noted slight dependence of  $d_{33}$  coefficients on pressure up to 50 kPa. When samples were exposed to 90 °C, the  $d_{33}$  value drops to 30% for 1 day. Also, an improvement in the  $d_{33}$  thermal stability was noted by preaging treatment. Again, in 2015, Zhang's group<sup>[51]</sup> prepared a piezoelectret film of IXPP foam, corona charged, and measured the  $d_{33}$  up to 650 pC N<sup>-1</sup> at a frequency of 200 Hz. For the  $d_{33}$  coefficient of 400 pC N<sup>-1</sup>, the figure of merit was found to be about 11.2 GPa<sup>-1</sup>. The VEH of these films is evaluated at varying load resistances and frequencies by means of one- and two-layer stacks. With a certain load resistance of 9 M $\Omega$  and at a frequency of 800 Hz, the maximum peak power was 120  $\mu$ W obtained for the single-layered IXPP film EH having a seismic mass 33.7 g and an area of 3.14 cm<sup>2</sup>. They reported that the power output further increased using two-layer IXPP film stacks in the electrical array. Recently, Sessler et al.<sup>[52]</sup> investigated a stacked and folded IXPP foam-based piezoelectret to study the effect of a number of layers and seismic mass on the performance of the EHs. The fabricated eight-layered-stacked foam showed a power of  $\approx 80$   $\mu$ W under a mass of 20 g, acceleration of 1 g, with a resistive load of 93 M $\Omega$ . More recently, Tefft<sup>[53]</sup> expanded the work by creating a more flexible foam stack of 20 layers and composite graphene electrodes, which resulted in the charging of a capacitor having a capacitance 1 mF at 1.025 V within 60 min at resonance 93 Hz and acceleration of 0.5 g. (Table 1)

**Polyethylene (PE)-Based Piezoelectrets:** Polyethylene (PE) is the most used commodity polymer in the world and piezoelectric applications of PE-based piezoelectrets would be significantly important as these materials are very attractive for the large-scale production of electret-based sensors and transducers due to their low cost and easy processing. Nakayama et al.<sup>[54]</sup> fabricated a porous PE (*p*-PE) piezoelectret film (thickness 30  $\mu$ m with porosity 58%).  $d_{33}$  was 80 pC N<sup>-1</sup>. Also, they found that

charges trapped in regions surrounding the film pores play a significant role. In another research, Tajitsu<sup>[55]</sup> fabricated the *p*-PE film using corona discharge for polarities treatment. They found a piezoelectric constant of 100 pC N<sup>-1</sup> in the perpendicular direction to their surface. Braña et al.<sup>[56]</sup> studied commercial PE foams with closed cells of 480  $\mu$ m using the thermal stretching process that involved simultaneous film heating to 100 °C and mechanical stretching, resulting in decreased film thickness and hence increased cell deformation. Further, when under corona discharge with an applied voltage 12 kV for 5 min, we end up with 170 pC N<sup>-1</sup> piezoelectric coefficient. Rychkov et al.<sup>[57]</sup> prepared low-density polyethylene (LDPE) based piezoelectrets via a template-based lamination method and reported the improvement in electret charge trapping, its thermal stability, and piezoelectricity when treated with orthophosphoric acid. Consequently, the  $d_{33}$  decay curves shift to a higher temperature by 40 °C.

Recently, Kaczmarek et al.<sup>[58]</sup> obtained MDPE films using extrusion and showed that cellular structures were formed when adding a foaming agent to films (Figure 6a). This enables build-up of electric charges, mostly at the cavity interfaces. The measured  $d_{33}$  (18 and 75 pC N<sup>-1</sup>) for a range of low stresses disappeared for larger stresses. For temperatures  $\approx 72$  and  $\approx 82$  °C, the appropriate activation energy reached 2.67 eV for a compacted sample and 3.28 eV for the noncompacted one. Hamdi et al.<sup>[59]</sup> produced the extrusion-blown, biaxially stretched cellular polymer films of linear low-density PE (LLDPE) and low-density PE (LDPE) and optimized the film cellular morphology for possible applications in piezoelectrets. They used a nucleating agent (talc) and a blowing agent (azodicarbonamide). Recently, Hamdi et al.<sup>[60]</sup> prepared this using same method,<sup>[59]</sup> followed by corona charging (Figure 6b). They showed that samples charged under nitrogen (N<sub>2</sub>) at 100 kPa had a better  $d_{33}$  coefficient than those charged under ambient air or N<sub>2</sub> at 20 kPa. Moreover, an optimized eye-like cellular structure with different aspect ratios (ARs) was obtained when imposed on two different thermal pressure treatments. They achieved higher  $d_{33}$  coefficients when the cell's structure elongated in both the transverse and longitudinal directions (higher AR). Further, the  $d_{33}$  coefficient of 935 pC N<sup>-1</sup> was found, which was best for AR-L (longitudinal AR) of 7.1, AR-T (transversal AR) of 4.6, and 0.52 relative foam density.  $d_{33}$  was further reported to increase to a maximum of 2550 pC N<sup>-1</sup> (Figure 6b) using a multilayered structure and reverse charging. Finally, the  $d_{33}$  value was much higher than for any PE and PP piezoelectrets reported so far. Again in 2019, the same group<sup>[61]</sup> fabricated cellular PE piezoelectrets using the same method and obtained very good  $d_{33}$  coefficients of 935 pC N<sup>-1</sup>. They showed a possible way to increase continuous service temperature (CST) resembling the PP-CST (i.e., 40–80 °C). Further, the  $d_{33}$  value was improved up to 3270 pC N<sup>-1</sup> with a three-layered film when reverse charged. Apart from its advantages such as ease of processibility and low price, it has drawbacks too, for example, a significantly low CST that limits a range of applications. This limitation can be overcome by making piezoelectrets from other higher-CST polymers (Table 2).

**Table 1.** Summary of various polyolefin (PP)-based single- and layered-cellular piezoelectrics.

Author	Polymer	$d_{33}$ [pC N <sup>-1</sup> ]	Layers	Output power	Highlights
Paajanen et al. (2001) <sup>[38]</sup>	PP	790	–	–	The highest $d_{33}$ was achieved after replacing air with N <sub>2</sub> gas inside the cellular structure.
Hillenbrand et al. (2003) <sup>[39]</sup>	PP	100–350 20 000	1-L 2-L>	–	–
Wegener et al. (2004) <sup>[40]</sup>	PP	306	–	–	–
Qiu et al. (2005) <sup>[42]</sup>	PP	350 215	–	–	SF <sub>6</sub> saturated Air saturated
Sborikas and Wegener (2013) <sup>[43]</sup>	PP	130	–	–	–
Anton et al. (2014) <sup>[44]</sup>	PP	175	–	6.0 μW	When EH was connected to 1 mF, it took 30 min to charge the capacitor up to 4.67 V.
Wu et al. (2015) <sup>[27]</sup>	PP	19 205	1-L <i>m</i> -L	52.8 mW m <sup>-2</sup>	A high-output voltage density of 13.7 V cm <sup>-2</sup> ; $d_{33}$ was found to be stable for many weeks at 60 °C.
Luo et al. (2015) <sup>[45]</sup>	PP	≈300 –	1-L 10-L	10.2 μW 100 μW	Ten-layer ferroelectrometer has 29.1 times the charging potential than the piezoelectret of one layer.
Mohebbi et al. (2017) <sup>[46]</sup>	PP	250, 550	–	–	$d_{33}$ was improved about >100% using N <sub>2</sub> in place of air as ionizing gas.
Mohebbi et al. (2017) <sup>[47]</sup>	PP	550, 800	–	–	$d_{33}$ coefficient of the treated PP film was improved by 45% as compared with the untreated sample.
Mohebbi and Rodrigue (2018) <sup>[48]</sup>	PP	800	–	≈1,824 pJ	When the air was replaced with N <sub>2</sub> , an improvement of 20% and 80% in the capacitance and stored energy of the samples, respectively, was noted.
Samadi et al. (2020) <sup>[49]</sup>	PP	–	–	84.02 mV N	Improvement in the piezoelectric performance of the foamed sample with thickness reduction; biocompatible and injection moldable.
Zhang et al. (2009) <sup>[50]</sup>	IXPP	400	–	–	$d_{33}$ values drop to 30% for 1 day exposed to temperature of 90 °C
Zhang et al. (2015) <sup>[51]</sup>	IXPP	650	1-L	120 μW	
Sessler et al. (2016) <sup>[52]</sup>	IXPP	–	8-L	80 μW	N <sub>2</sub> saturated
Tefft (2018) <sup>[53]</sup>	IXPP	–	20-L with composite graphene electrodes	–	1 mF capacitor charged to 1.025 V within 60 min at resonance 93 Hz and 0.5 g acceleration.

### 3.1.2. Polyester-Based Piezoelectric Foams

**Polyethylene Terephthalate (PET)-Based Piezoelectrets:** The concept of polyolefin (PP and PE)-based piezoelectrets can be effectively utilized in the fabrication of polyester polymers. First, polyester piezoelectrets were made from commercially produced PET foams, studied by Wegener et al.<sup>[62]</sup> in 2005. They investigated the piezoelectricity of the foam-structured PET film with 160 ± 10 μm thickness and a density range of 0.37 and 0.40 g cm<sup>-3</sup>. The samples were then annealed in the temperature range of 70 and 160 °C for 16 h that resulted in a reduction in void height and the elastic modulus and an enhancement in film density. For example, when the film thickness reduced to ≈70 μm, the density enhanced from ≈0.4 to ≈0.66 g cm<sup>-3</sup>. The samples were then charged through the application of voltages in range –27 and –60 kV for 30 s in N<sub>2</sub> saturation at 6 bars

charged further. The samples on both surfaces were metalized by Al electrodes of 50 nm thickness. A maximum  $d_{33}$  of 23 pC N<sup>-1</sup> for sample density of 0.67 g cm<sup>-3</sup> was obtained at ≈110 °C constant temperature. Wirges et al.<sup>[63]</sup> used the same fundamental concepts developed for optimizing cellular PP piezoelectrets by Wegener et al.<sup>[64]</sup> and investigated the piezoelectricity of PET. The authors obtained the cellular structure via foaming using scCO<sub>2</sub> and then biaxially stretched up to 150% at 230 °C and hence N<sub>2</sub> inflation occurred for 2 h at 230 °C (**Figure 7a**). The samples were then saturated with SF<sub>6</sub> and corona charged by applying voltages ranges from –20 to –60 kV for 60 s at 3 bars of pressure. The measured  $d_{33}$  coefficient was up to 500 pC N<sup>-1</sup> when a 3.0 N static force was applied followed by a 1 N dynamic force at 2 Hz frequency (**Figure 7b**).

**Polyethylene Naphthalate (PEN)-Based Piezoelectrets:** Polyethylene naphthalate (PEN) is a thermoplastic polyester, another

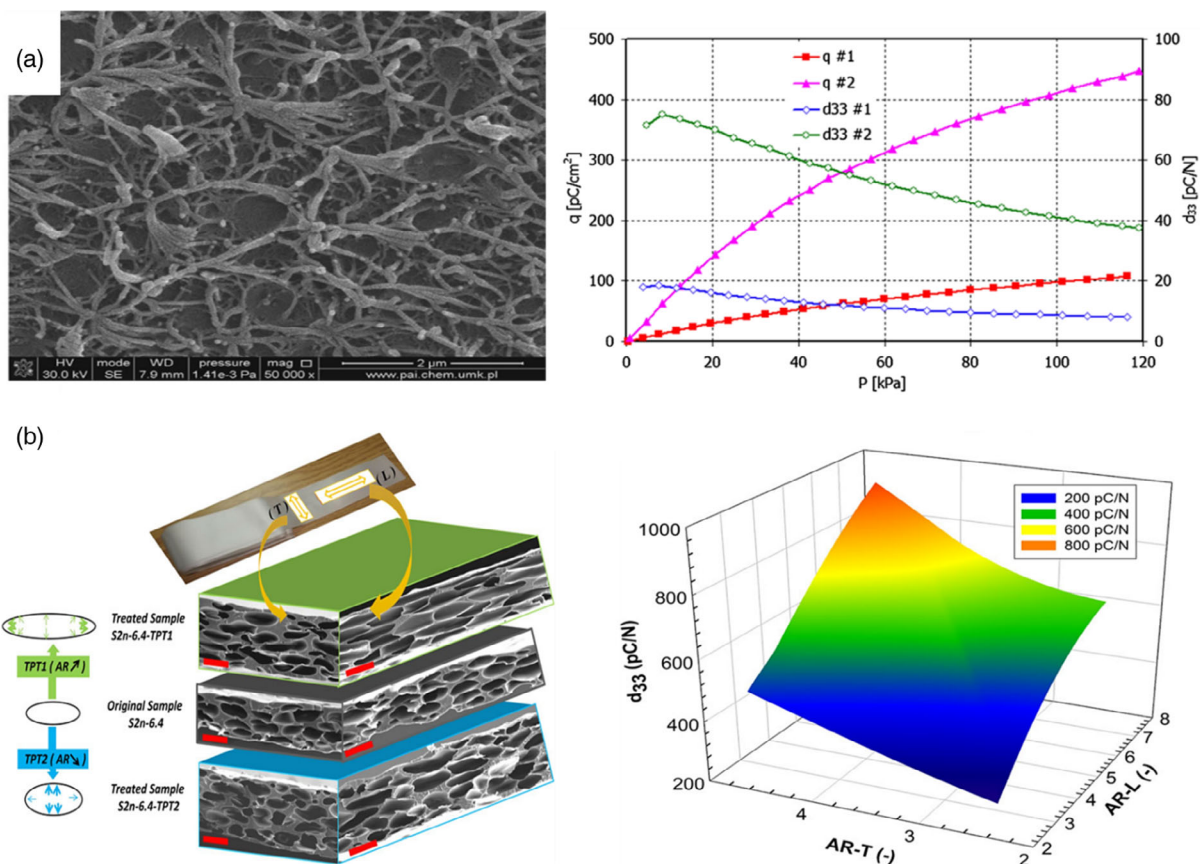


**Figure 6.** a) SEM images of blown, extruded MDPE film: cross section of the MDPE film after additional compacting at 140 °C; dependence of charge density and piezoelectric constant  $d_{33}$  versus stress. Reproduced with permission.<sup>[58]</sup> Copyright 2017, The Springer Nature. b) Typical structures of the original and TPT samples (S2n-6.4). Red lines represent a 100 μm scale. Relationships between the piezoelectric coefficient ( $d_{33}$ ) and the AR in both longitudinal (AR-L) and transversal (AR-T) directions. Reproduced with permission.<sup>[60]</sup> Copyright 2018, Wiley-VCH GmbH.

**Table 2.** Summary of various PE-based single- and layered cellular piezoelectrics.

Author	Polymer	$d_{33}$ (pC/N)	Layers	Output power	Highlights
Nakayama et al. (2009) <sup>[54]</sup>	PE	80	–	–	–
Tajitsu (2011) <sup>[55]</sup>	PE	100	–	–	Corona charged
Braña et al. (2011) <sup>[56]</sup>	PE	170	–	–	Thermally stretched and corona charged
Rychkov et al. (2012) <sup>[57]</sup>	LDPE	≈30–38	–	–	Fabricated via template-based lamination method. Treatment with orthophosphoric acid. Reproduced good thermal stability.
Kaczmarek et al. 2017 <sup>[58]</sup>	MDPE	18–75	–	–	
Hamdi et al. (2018) <sup>[59]</sup>	LLDPE LDPE	–	–	–	Fabricated via extrusion blowing. The cellular morphology of biaxially stretched PP film is optimized.
Hamdi et al. (2019) <sup>[60]</sup>	LLDPE LDPE	935 2550	1-L 3-L	–	Sample charged in N <sub>2</sub> has better $d_{33}$ than charged in air; $d_{33}$ value was much higher than any PE or PP, reported so far.
Hamdi et al. (2019) <sup>[61]</sup>	LLDPE LDPE	935 2550	1-L 3-L	–	A possibility in increasing, resembling CST of PP.



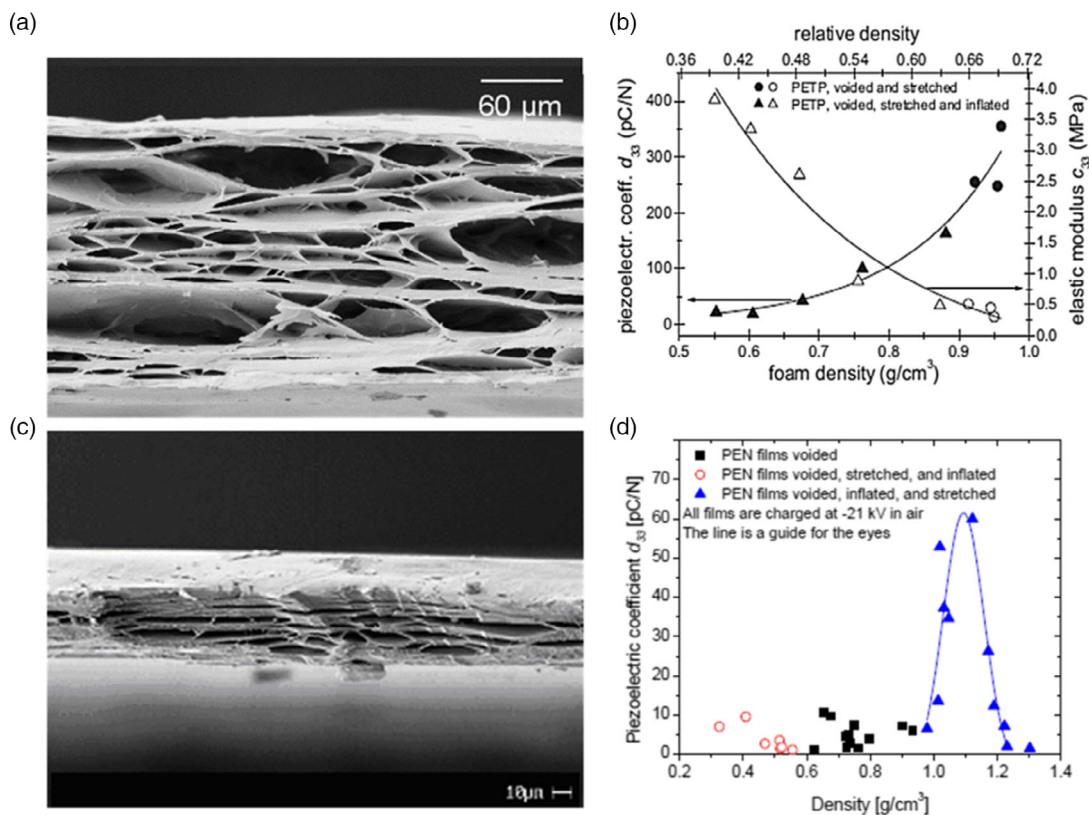


**Figure 7.** PET: a) The SEM image of a voided, stretched, and an inflated PET film. b)  $d_{33}$  (piezoelectric coefficient) (full symbols) and  $c_{33}$  (elastic moduli) (open symbols) of the voided and stretched PET film (circles) and voided, stretched, and inflated PET film (triangles). Reproduced with permission.<sup>[63]</sup> Copyright 2007, Wiley-VCH GmbH; PEN: c) Voided, inflated, and stretched PEN film. d)  $d_{33}$  as a function of film density.<sup>[65]</sup> Reproduced with permission.<sup>[65]</sup> Copyright 2008, Walter de Gruyter GmbH.

high-performance polymer that garnered additional attention due to its same chemical structure as PET, with the only exception being the double-ring naphthalate replacing the single-ring terephthalate, making it have better mechanical, thermal, and barrier characteristics in comparison with PET. PEN piezoelectrets were recently created effectively and offered promising results, such as reasonably good thermal stability for piezoelectric capabilities or a comparatively strong “Curie relaxation” in the range of 80–100 °C.<sup>[65]</sup>

Fang et al.<sup>[66]</sup> reported cellular PEN piezoelectrets fabricated from commercial uniform polymer films, which were foamed in  $\text{scCO}_2$ , inflated, biaxially stretched, electrically charged, and metalized. They measured  $d_{33}$  coefficients up to  $140 \text{ pC N}^{-1}$  and demonstrated the feasibility of these cellular PEN films to be used as transducers. They also found that piezoelectricity of these piezoelectrets is only partly stable at high temperatures up to 100 °C. Further in 2008, the same group of Fang<sup>[65]</sup> proposed a preparation process for cellular PEN films which involved foaming using  $\text{scCO}_2$ , controlled inflation via gas diffusion, expansion, and finally biaxial stretching (Figure 7c). The PEN films were foamed by soaking them in supercritical  $\text{CO}_2$  at ambient temperature for a few hours at a pressure of up to 100 bar. Only samples with the right density range and optimum cellular architectures have high electromechanical responses,

that is, substantial piezoelectric thickness coefficients. The highest  $d_{33}$  of  $\approx 60 \text{ pC N}^{-1}$  was measured for the sample density of  $\approx 1.0 \text{ g cm}^{-3}$  (Figure 7d). Fang et al.<sup>[67]</sup> prepared PEN piezoelectrets using process voiding, inflation, and stretching and reported a significant increase in  $d_{33}$  with charging voltage and found its saturated value of  $\approx 45 \text{ pC N}^{-1}$  at  $\approx 8.5 \text{ kV}$ . The maximum  $d_{33}$  of  $\approx 80 \text{ pC N}^{-1}$  was noted when charged at room temperature, at 80 °C as well as at 100 °C (Table 3).

### 3.1.3. Fluoropolymer-Based Piezoelectric Foams

**Polytetrafluoroethylene (PTFE)-Based Piezoelectrets:** Polytetrafluoroethylene (PTFE)-based piezoelectrets are significant because of their extraordinary charge storage and good thermal stability properties. Gerhard-Multhaupt et al.<sup>[68]</sup> fabricated novel porous PTFE films by corona charging (positively or negatively) at room or higher temperatures and investigated the charge storage property compared with nonporous polymer samples using isothermal surface potential measurements. They noted enhanced stability in surface charge for both polarities due to porosity. They also studied both the direct and indirect piezoproperties of layered (single, double, and quadruple) samples through quasistatic and acoustical–transducer measurements, respectively, and measured  $d_{33}$  of  $600 \text{ pC N}^{-1}$ . Finally, the value

**Table 3.** Summary of various polyester-based single- and layered cellular piezoelectrics.

Author	Polymer	$d_{33}$ (pC/N)	Layers	Output power	Highlights
Wegener et al. (2005) <sup>[62]</sup>	PET	23	–	–	N <sub>2</sub> saturated.
Wirges et al. (2007) <sup>[63]</sup>	PET	500	–	–	SF <sub>6</sub> saturated and corona charged
Fang et al. (2007) <sup>[66]</sup>	PEN	140	–	–	Partial stability of piezoelectricity at high temperatures up to 100 °C
Fang et al. (2008) <sup>[65]</sup>	PEN	60	–	–	Showed electromechanical response ( $d_{33}$ ) as a function of film density. Highest $d_{33}$ found for density 1 g cm <sup>-3</sup> .
Fang et al. (2010) <sup>[67]</sup>	PEN	10-80	–	–	$d_{33}$ increased with the charging voltage

of  $d_{33}$  was one order of magnitude higher than the conventional piezopolymers, providing extra potential for many device applications. Hillenbrand et al.<sup>[39]</sup> investigated piezoelectricity in cellular PP with thickness from 50 to 100  $\mu\text{m}$  in the structure of bilayers or multilayers composed in the solid or voided form including an extra air layer. The  $d_{33}$  of the cellular PP was of the order of 100–350 pC N<sup>-1</sup>. The  $d_{33}$  of bilayer or multilayer structured samples was significantly larger, reaching up to 20 000 pC N<sup>-1</sup> in some cases. Also, a decrease toward larger frequencies was noted for the single-layer sample.

Zhang et al.<sup>[69]</sup> introduced two ways for the preparation of cellular piezofluorocarbon polymers and prepared laminated films of PTFE and FEP. In method 1, they fused compact FEP and PTFE layers with the application of mechanical pressure by a metal mesh at above-FEP melting temperatures and both polymers worked as charge storage dielectrics. However, in method 2, compact FEP and porous PTFE layers fused at higher temperatures by application of force without any metallic mesh and FEP worked as the main charge storage dielectric, and porous PTFE functioned as the cavity. A quasistatic  $d_{33}$  coefficient in the range of 500 and 2200 pC N<sup>-1</sup> was measured, which was independent of static pressure up to 20 kPa. They also noted higher values of  $d_{33}$  and better thermal stability than cellular PP piezoelectrets. In 2009, Zhang et al.<sup>[70]</sup> prepared voided-structured PTFE films through a sintering procedure and corona charge to achieve piezoelectricity. A quasistatic  $d_{33}$  coefficient of 250 pC N<sup>-1</sup> resulted from a compact, layered, and biaxial-tension porous sample. Also, the preaging treatment of samples was studied and lowering of  $d_{33}$  was noted as 2% per day at 120 °C. Therefore, an improvement in the thermal stability by preaging came out as an effective technique. Zhang et al.<sup>[71]</sup> used commercial three-layered PTFE films composed of two skin layers of dense PTFE ( $\approx 20 \mu\text{m}$ ) and a film of cellular PTFE (100–250  $\mu\text{m}$ ) placed in the center and the sample system corona was charged at a -25 kV potential for 60 s followed by skins' metallization by thin Al layers. They performed a quasistatic measurement by application of a force of 1.96 N to the sample for a long time and then the force removed and measured generated charge for 10 s using an electrometer. The  $d_{33}$  coefficient range was 1000–2700 pC N<sup>-1</sup> and found during initial quasistatic measurements. They also reported the stabilization of  $d_{33}$  coefficients and reached 75%, 40%, and 25% of their starting values after annealing for 1500 min at temperatures of 90, 120, and 150 °C, respectively.

**Fluorinated Ethylene-Propylene (FEP)-Based Piezoelectrets:** The copolymer fluorinated ethylene propylene (FEP) has better chemical, physical, and electrical characteristics that make it capable of potential applications for temperatures around or slightly higher than 100 °C.<sup>[72]</sup> Apart from these, while the production of regular cellular structures with controlled shape is technically problematic and difficult, the use of the polymer layer system or sandwich-based piezoelectrets was proposed for making the process of fabrication easier.<sup>[31,73]</sup> FEP is a thermoplastic copolymer and melt processable opposite to PTFE homopolymer.

Veronina et al.<sup>[74]</sup> adopted the same procedure as used for polyester foaming method with scCO<sub>2</sub> and fabricated the FEP foams by generating a single big void across the thickness of the film. A  $d_{33}$  coefficient up to 50 pC N<sup>-1</sup> reported the cellular FEP piezoelectrets after charging and electrode evaporation.

Zhang et al.<sup>[75]</sup> fabricated layered electret films based on FEP copolymer via template patterning, fusion bonding, and contact charging. They showed  $d_{33}$  ranging from 1000 to 3000 pC N<sup>-1</sup>, and an improvement in thermal stability after annealing the systems at 120 °C.

In another study, Zhang et al.<sup>[73]</sup> used the same method and fabricated the layered piezoelectret film based on FEP having a crosstunnel structure. They measured  $d_{33}$  coefficient in the range of 1000–3700 pC N<sup>-1</sup>, and after annealing at 125 °C, the system's sensitivity stabilized and retained 40% of its initial value. They also created a micro-EHG (4.3 cm<sup>2</sup>) with a seismic mass of 69.5 g and measured the output power of  $\approx 0.5 \mu\text{W}$  when subjected to a frequency up to 120 Hz and 1 g acceleration.

In 2016, Wang et al.<sup>[28]</sup> fabricated porous layered piezoelectrets comprising two dense fluorinated ethylene propylene (dFEP) skin layers and a fibrous single inner porous PTFE (fPTFE) layer via the hot-pressing method at temperature of  $\approx 285 \text{ °C}$  and pressure of  $\approx 5 \text{ MPa}$  and, further, metalized and corona poled. Electret generator based on the fabricated film showed a maximum peak power density of  $\approx 31.4 \mu\text{W cm}^{-2}$  with a load resistance of 40 M $\Omega$ . Moreover, the application of the electret generator for a self-powered human breathing sensor was also demonstrated. In 2017, Wang<sup>[76]</sup> reported an extremely sensitive microcellular fluorocarbon-based piezoelectret fabricated via a three-step hot-pressing method using double layer of FEP/f-PTFE with a single central layer of FEP and two stainless steel plates as skin layers. They measured a remarkable  $d_{33}$  of 7380 pC N<sup>-1</sup>, a lower response time of 50 ms, higher stability

of 30 000 cycles, and a considerably lower limit of detection of  $\approx 5$  Pa when configured as a pressure sensor in the pressure of  $< 1$  kPa.

In 2018, Zhang et al.<sup>[77]</sup> fabricated the ferroelectric nanogenerator based on laminated fluorinated ethylene propylene (FEP) using laminated tunnel films having wide voids in between them. They obtained a better voltage coefficient of  $g_{31} = 3 \text{ V m N}^{-1}$  equivalent to  $d_{31} = 32 \text{ pC N}^{-1}$  in the transverse direction. A high voltage coefficient because of the lower permittivity of this material system as compared with the PVDF of around  $g_{31} \approx 0.2$  enables it to be the best candidate for EH applications. A lightweight EH having a dimension of  $3 \times 5 \times 8 \text{ mm}^3$  was developed and the output power was found as  $50 \mu\text{W}$  with a seismic mass of 0.09 g at acceleration 1 g.

In another study, Shi et al.<sup>[78]</sup> presented a unique and straightforward way to prepare a sandwich structure and used a porous foam layered between two FEP films with aluminum electrodes on upper and lower layers (Figure 8a,b). They measured  $d_{33} \approx 1000 \text{ pC N}^{-1}$  and when used as the EH, generated  $6.4 \mu\text{W}$  output power. The principle of generation of piezoelectricity is given in Figure 8c. Also, the experimental coupling coefficient was achieved as 0.107, and a capacitor of value  $10 \mu\text{F}$  was configured with the system and charged up to 0.2 V within 40 s.

Recently, Ma et al.<sup>[79]</sup> fabricated unipolar FEP piezoelectrets using a three-step procedure (wavy FEP film preparation via the template method, negative corona charging of the wavy film, and bonding with another uncharged wavy FEP film). They reported a maximum output a power of  $\approx 355 \mu\text{W}$  for an EH ( $30 \text{ mm} \times 10 \text{ mm}$ ) applied at frequency 22 Hz when the acceleration and seismic mass was  $1 \times \text{g}$  and 3 g, respectively. The thermal stability improvement using negatively charged unipolar FEP piezoelectrets was also noted. More recently, Ben Dali et al.<sup>[80]</sup> presented a VEH based on FEP piezoelectrets

functioning in the  $d_{31}$  mode and fabricated in the form of a parallel tunnel structure by fusing together two FEP films with well-defined air gaps. The reported  $g_{31}$  was  $\approx 0.7 \text{ V m N}^{-1}$ . An air-spaced cantilever arrangement fabricated via the additive manufacturing technique and analyzed by exposing it to a shaker generated sinusoidal vibrations with acceleration. They measured an output normalized power of  $320 \mu\text{W}$  at  $\approx 35$  Hz and seismic mass of 4.5 g at acceleration 0.1 g. They demonstrated a significant improvement of air-spaced VEH as compared with previously reported polymer-based cantilever devices.

*Amorphous Teflon (AF)-Based Piezoelectrets:* The advantage of using Teflon AF in creating piezoelectrets is that it can process easily compared with other types of fluoropolymers besides easy dissolution in a perfluorocarbon solvent, which gives the possibility to produce films through the spin-coating and drop-casting techniques. Mellinger et al.<sup>[81]</sup> produced the AF-based porous films of 3–10  $\mu\text{m}$  thickness. To get a desired average thickness, many layers were drop cast on one another. Then, it was corona charged, and the measurements showed that the piezoelectrets of Teflon AF exhibited large piezoelectricity ( $d_{33}$ :  $\approx 600 \text{ pC N}^{-1}$ ). The stability of piezosensitivity was noted at 120 °C.

Wang et al.<sup>[82,83]</sup> made Teflon AF piezoelectrets on a microcellular PDMS structure using a microfabrication procedure. They fabricated the sample by casting the multilayered PDMS and stacking (Figure 9i). A photoresistive mold was formed on a Si wafer. A thin PDMS layer was imitated using the cellular microstructure and cast on the mold top. A closed cavity-PDMS foam was obtained via bonding both the patterned film and a blank thin layer. Further, by repeating both processes (repeating the casting), a multilayered structure could be formed. The voids may be filled with the Teflon AF solution, which was then evaporated, depositing a thin AF film layer which gives great charge storage after being charged. Figure 9ii shows the SEM

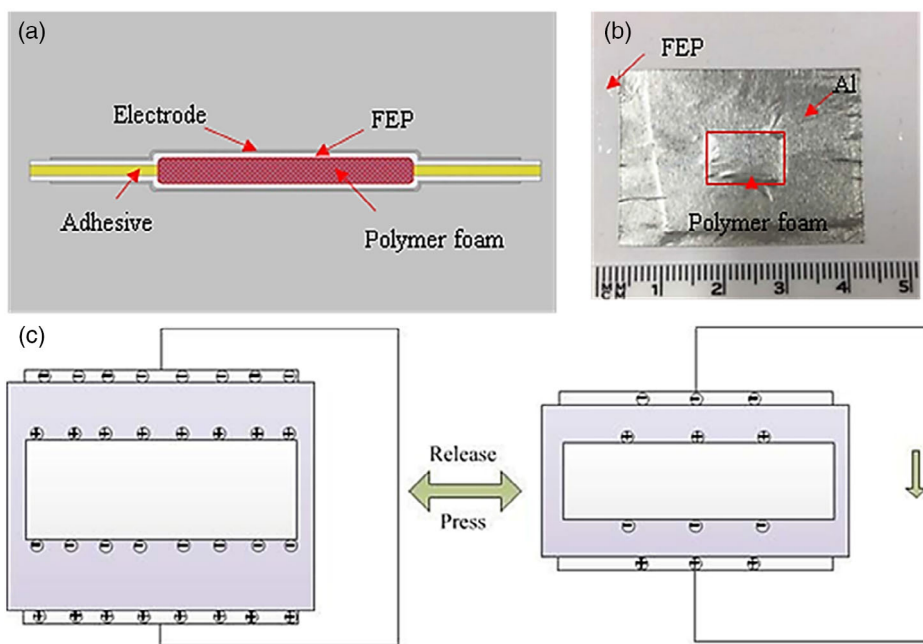


**Figure 8.** Stacked or layered FEP porous polymer-based piezoelectrets: a) Schematic. b) Digital photograph. c) Working principle. Reproduced with permission.<sup>[78]</sup> Copyright 2018, IOP Publishing Ltd.

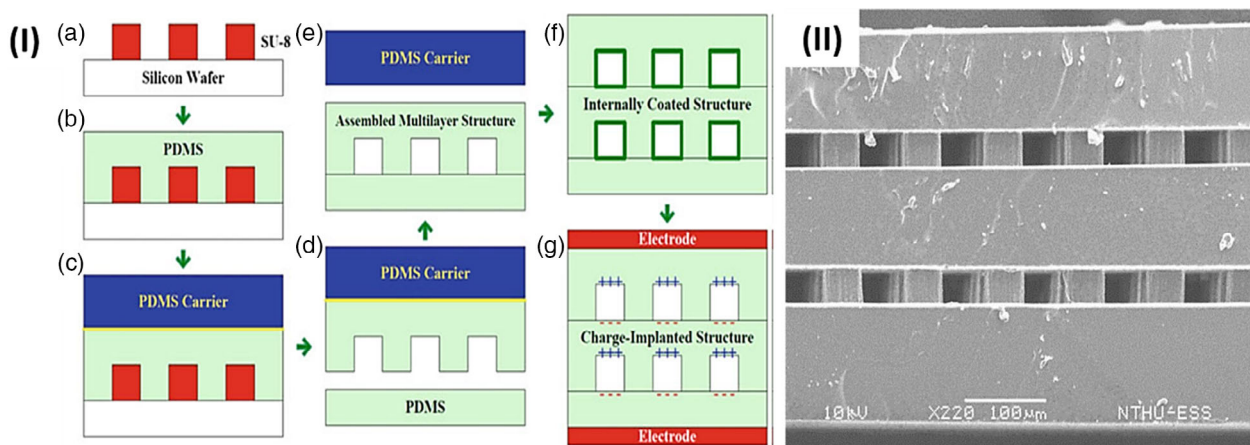


**Figure 9.** i) Schematic illustration of the microfabrication of PDMS piezoelectrets. Reproduced with permission.<sup>[82]</sup> Copyright 2012, IOP Publishing Ltd. ii) SEM image of microfabricated cellular PDMS. Reproduced with permission.<sup>[83]</sup> Copyright 2013, IOP Publishing Ltd.

image of the sample cross section. When the sample was electrode deposited and charged, it showed a  $d_{33}$  coefficient greater than  $1000 \text{ pC N}^{-1}$  (Table 4).

### 3.1.4. Other Polymer-Based Piezoelectric Foams

**Cyclo-Olefin Polymer (COP) and Copolymer (COC)-Based Piezoelectrets:** Cyclo-olefin polymers (COPs) present a good electret property as well as excellent charge stability.<sup>[84]</sup> As a result, they are potential piezoelectret materials. The COPs and other olefin polymers were blended to lower glass transition temperature ( $T_g$ ) to improve the elastic properties and hence the processability of polymers. Stretching filler-loaded polymer compounds creates cellular film formations. When compared with cellular PP foams, the temperature window was quite limited. The cavity dimension was optimized using gas diffusion expansion (GDE) methods. The cellular COP piezoelectrets have piezoelectric  $d_{33}$  coefficient of  $\approx 15 \text{ pC N}^{-1}$ . In comparison with cellular PP piezoelectrets, the  $d_{33}$  coefficient is rather low. Despite this, the piezoelectric sensitivity of COP piezoelectrets is significantly superior to that of cellular PP and polyester piezoelectrets up to  $110^\circ\text{C}$ .<sup>[85,86]</sup>

In 2013, Li and Zeng<sup>[87]</sup> proposed the  $\text{scCO}_2$ -assisted COC film fabrication for producing a regular cell structure. Because of the powerful COC– $\text{CO}_2$  interactions, when the COC film was exposed to  $\text{scCO}_2$ , the surface glass transition temperature dropped dramatically below that of the bulk, which resulted in near-surface polymer chains that are substantially more mobile and diffusive. **Figure 10a** depicts the sample preparation process schematically. They used five-layer COC film stacks. Regular rectangular slots were carved using a  $\text{CO}_2$  laser in two of the five films. The carved slots have the same length and breadth, as well as the spacing between them was the same. Every three films were separated using the two films with openings, and the pattern was then shifted by half of the total width of the opening and the spacing, as shown in **Figure 10a**. The stack was then treated in  $\text{CO}_2$  with a temperature of  $120^\circ\text{C}$  at  $10 \text{ MPa}$  pressure for 12 h. Good bonding was achieved between the interfaces. In this method, bulk deformation was prevented because the

temperature was lower than the bulk  $T_g$ . These were big advantages when comparing with other methods utilizing fusion bonding, where thermal degradation and deformation of the system structures were huge concerns. They also realized the sample compression by unit cell bending and achieved significant piezoelectricity, noting the  $d_{33}$  coefficient from 100 to  $1000 \text{ pC N}^{-1}$  with thermal stability up to  $110^\circ\text{C}$  (**Figure 10b**).

**Polycarbonate (PC)-Based Piezoelectrets:** Polycarbonate (PC) is a hard thermoplastic with a strong creep modulus that also has an outstanding dimensional stability heat resistance and electrical insulating qualities. PC is frequently utilized in electrical applications due to these characteristics, such as a capacitor dielectric with great stability.

Excellent charge stability of the PC films having additives after thermal treatment was reported.<sup>[88]</sup> In 2010, Behrendt<sup>[89]</sup> successfully prepared foamed PC via foaming using  $\text{scCO}_2$ , as well as stretching a composite film containing fillers, which were removed by phase extraction.

The PC foams were corona charged with a voltage of  $+32 \text{ kV}$ . However, this method cannot be used to generate piezoelectricity in PC foams. This may be because of their thickness for effective charging and/or the films were greatly stiffened to bend enough when subjected to mechanical or electrical stress. In another study, Qiu et al.<sup>[90]</sup> proposed a new method for the fabrication of PC piezoelectrets. They used the computer-controlled laser cutting and prepared a grid of double-sided adhesive tape having pattern-desired opening. Two PC films metalized on one surface were then joined using the grid via their surfaces with nonmetalized surfaces, forming a well-defined cavity around the grid openings. A  $d_{33}$  coefficient up to  $30 \text{ pC N}^{-1}$  was noted when contact charged with  $2 \text{ kV}$ .

In 2014, Sborikas et al.<sup>[91]</sup> proposed another method in which they prepared PC piezoelectrets via screen printing. A  $d_{33}$  coefficient up to  $30 \text{ pC N}^{-1}$  which was thermally stable up to  $100^\circ\text{C}$  was measured when charged.

**Polydimethylsiloxane (PDMS)-Based Piezoelectrets:** In 2014, McCall et al.<sup>[92]</sup> synthesized the foam based on piezoelectric polymer composites using different sugar-templating techniques with the inclusion of sugar grains directly into mixtures of

**Table 4.** Summary of various fluoropolymer-based single- and layered cellular piezoelectrets.

Author	Polymer	$d_{33}$ [pC N <sup>-1</sup> ]	$g_{33}$ [Vm N <sup>-1</sup> ]	Layers	Output power	Highlights
Gerhard-Mulhaupt et al. (2000) <sup>[68]</sup>	PTFE	600	–	–	–	–
Hillenbrand et al. (2003) <sup>[39]</sup>	PTFE	20 000	–	2-L to <i>m</i> -L	–	–
Zhang et al. (2007) <sup>[69]</sup>	FEP-cPTFE-FEP	500–2200	–	3-L	–	–
Zhang et al. (2009) <sup>[70]</sup>	PTFE	250	–	–	–	A lowering of $d_{33}$ was noted 2% per day at 120 °C.
Zhang et al. (2013) <sup>[71]</sup>	dPTFE-cPTFE-dPTFE	1000–2700	–	3-L	–	Stabilization of $d_{33}$ coefficients and it reached 75%, 40%, and 25% of their starting values after the annealing for 1500 min at temperatures of 90, 120, and 150 °C, respectively.
Zhang et al. (2014) <sup>[73]</sup>	FEP	1000–3700	–	2-L	≈0.5 μW	Created a micro-EHG (4.3 cm <sup>2</sup> ) with a secondary Mass of 69.5 g and it was subjected to a frequency up to 120 Hz and 1 g acceleration.
Veronina et al. 2008 <sup>[74]</sup>	FEP	50	–	–	–	–
Zhang et al. (2012) <sup>[75]</sup>	FEP	1000–3000	–	2-L	–	Good thermal stability at 120 °C.
Wang et al. (2016) <sup>[28]</sup>	dFEP/fPTFE/dFEP	–	–	3-L	31.4 μW cm <sup>-2</sup>	Max. charge density was measured as ≈9.39 nC cm <sup>-2</sup> ; can be useful in the self-powered human breathing sensor.
Wang et al. (2017) <sup>[76]</sup>	FEP/fPTFE-FEP- fPTFE/FEP	7380	–	5-L	–	The max. surface charge density of 7.54 μC m <sup>-2</sup> was noted at applied periodic pressure of ≈1 kPa.
Zhang et al. (2018) <sup>[77]</sup>	FEP	$d_{31} \approx 32$	$g_{31}$	–	50 μW	EH (3 × 5 × 8 mm <sup>3</sup> ) was developed and the output power was found as 50 μW with a secondary mass of 0.09 g under the acceleration of 1 g.
Shi et al. (2018) <sup>[78]</sup>	FEP	1000	–	2-L	6.4 μW	A capacitor of 10 μF was charged up to 0.2 V within 40 s.
Ma et al. (2019) <sup>[79]</sup>	w-FEP	–	–	2-L	355 μW	Output power was found comparable with the best bipolar EHs; unipolar charging was reported as simplest way to gain thermal stability.
Ben Dali et al. (2020) <sup>[80]</sup>	FEP	–	0.7	2-L	320 μW	Demonstrated a significant improvement of air-spaced VEH.
Mellinger et al. (2001) <sup>[81]</sup>	AF	600	–	–	–	The stability of piezosensitivity was noted at temperature 120 °C
Wang et al. (2012) <sup>[82]</sup>	AF on cPDMS	>300	–	<i>m</i> -L	–	A thin AF film layer gave great charge storage capacity after being charged.
Wang et al. (2013) <sup>[83]</sup>	AF	>1000	10 mV Pa <sup>-1</sup>	–	–	An input pressure of 1 Pa resulted in voltage output of 10 mV.

polydimethylsiloxane (PDMS) comprising carbon nanotubes and barium titanate nanoparticle (NPs); then, sugar removal occurred after polymer curing. The mass ratio of sugar and polymer adjusted and tuned the elasticity and porosities. The direct relationship between piezoelectric outputs and porosity showed electrical performance associated with the foams; using this, the researcher achieved a piezoelectric coefficient of value of ≈112 pC N<sup>-1</sup> and a power output of ≈18 mW cm<sup>-3</sup> under a load of 10 N for the sample of highest porosity. Furthermore, these novel materials found a wide application in areas such as biosensors, acoustic actuators, and energy scavenging systems.

Recently in 2016, Kachroudi et al.<sup>[93]</sup> prepared microcellular PDMS piezoelectret via a molding process, charged with triangular voltages (1 and 4 kV) at 0.5 Hz frequency, and measured a  $d_{33}$  of ≈350 pC N<sup>-1</sup> when charged at room temperature. Further, they reported that poling at a higher temperature increases

the  $d_{33}$  thermal stability at a cost of a reduction in piezoelectric performance.

**PVDF-Based Piezoelectrets:** The fabrication of PVDF foam having complex 3D geometry with excellent piezoelectricity with high power density has now become a great global challenge. In 2011, Cha et al.<sup>[94]</sup> presented a novel nanoporous PVDF-based piezoelectret fabricated via the nanowire-assisted template method and demonstrated that porous PVDF-based nanogenerators could produce power density of ≈0.17 mW cm<sup>-3</sup>. The piezoelectric properties of the nanogenerator (1 cm × 1 cm × 5 μm) were measured under the sonic input (100 dB and 100 Hz) and reported open circuit (OC) voltage(p-p) of 2.6 V and SC current(p-p) of 0.6 μA.

More recently, in 2019, Jahan et al.<sup>[95]</sup> prepared a cellular PVDF piezoelectret via conventional process extrusion, stretching, inflation, and corona charging. They investigated the effect of CO<sub>2</sub> gas inflation treatment using different gas diffusion (GD)

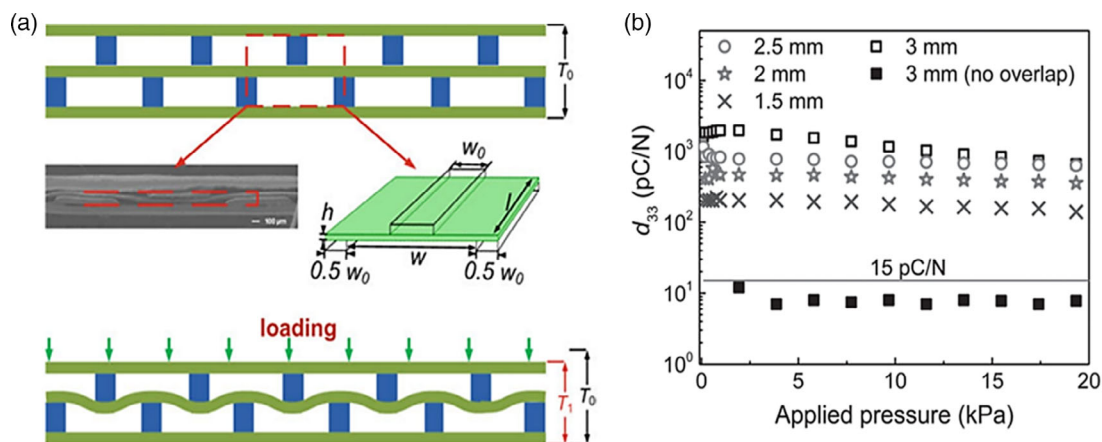


**Figure 10.** a) The preparation method for COC film systems with the regular cavity structure is illustrated in this diagram. b) Quasistatic piezoelectric  $d_{33}$  coefficient of a series of COC piezoelectret samples with different designs as shown in figure a. The horizontal line ( $15 \text{ pC N}^{-1}$ ) denotes the performance level of the COC piezoelectrets reported from past literature.<sup>[64,85]</sup> Reproduced with permission.<sup>[87]</sup> Copyright 2013, Wiley-VCH GmbH.

inflation or expansion processes compared with the results of  $\text{N}_2$  inflation, as reported by their previous research. The  $d_{33}$  coefficient of  $\text{CO}_2$ -inflated samples ( $327 \text{ pC N}^{-1}$ ) was found to be 30% higher compared with  $\text{N}_2$ -inflated samples ( $251 \text{ pC N}^{-1}$ ) when stepwise pressure was applied.

**Polylactic Acid (PLA)-Based Piezoelectrets:** Recently in 2020, Zhukov et al.<sup>[96]</sup> prepared new biodegradable cellular piezoelectret films of PLA and presented the preliminary measured outcomes of both its fabrication and piezoelectricity measurements. They followed the classical method for piezoelectret preparation such as microstructure alteration using  $\text{CO}_2$ -hot pressing-corona charging. **Figure 11b,d** shows the SEM images of cross sections from the original PLA foam and hot-pressed

PLA foam. Large  $d_{31}$  ( $\approx 44 \text{ pC N}^{-1}$ ) and  $d_{33}$  ( $600 \text{ pC N}^{-1}$ ) coefficients were measured under the quasistatic mode for the  $360 \mu\text{m}$ -thick film with porosity of  $\approx 60\%$  (Figure 11a,c). Also, after 20 days of being poled, the piezoresponse decreased to half of its first measured value, but after a long time, it became constant. The great biocompatibility features and ecofriendly nature of PLA-based piezoelectrets open a broad range of biological applications (micro-EHs [MEHs], biosensors, etc.) (Table 5).

### 3.2. Cellular Piezoelectric Composites

Polymeric cellular composites have many specific properties such as low specific weight, strong temperature resistance,

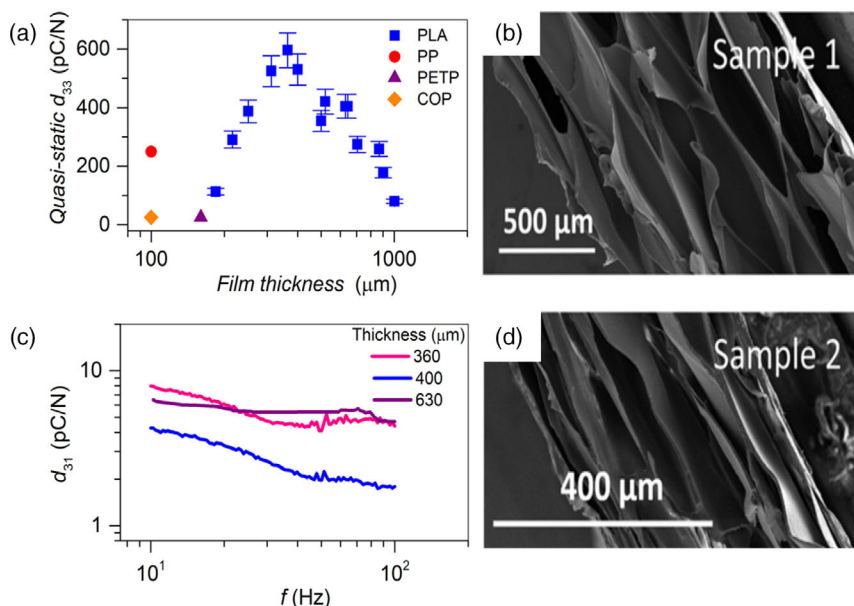


**Figure 11.** a) A comparison of the  $d_{33}$  coefficients of PLA foams with varying thickness and some reported piezoelectrets in the past. c)  $d_{31}$  coefficient as a function of frequency for PLA piezoelectrets' different thicknesses under a dynamic force of  $0.2 \text{ N}$ . b,d) SEM images of cross sections from sample-1 (original PLA foam) and sample-2 (hot-pressed PLA foam). Reproduced with permission.<sup>[96]</sup> Copyright 2020, AIP Publishing.

**Table 5.** Summary of various other polymers-based single and layered piezoelectrets.

Author	Polymer	$d_{33}$ [pC N <sup>-1</sup> ]	$g_{33}$	Layers	Output power	Highlights
Li and Zeng 2013 <sup>[87]</sup>	COC	100–1000	–	5-L	–	$d_{33}$ thermally stable upto 110 °C.
Behrendt (2010) <sup>[89]</sup>	PC	–	–	–	–	–
Qiu et al. 2010 <sup>[90]</sup>	PC	30	–	–	–	Fabricated via computer-controlled laser cutting.
Sborikas et al. (2014) <sup>[91]</sup>	PC	30	–	–	–	Fabricated via screen printing; Thermally stable up to 100 °C when charged.
McCall et al. (2014) <sup>[92]</sup>	PDMS	112	–	–	18 mW cm <sup>-3</sup>	Fabricated via sugar-templating techniques
Kachroudi et al. (2016) <sup>[93]</sup>	PDMS	≈350	–	–	–	Poling at higher temperature increases the $d_{33}$ thermal stability at a cost of reduction in piezoelectric performance.
Cha et al. (2011) <sup>[94]</sup>	npPVDF	–32.5	–	–	≈0.17 mW cm <sup>-3</sup>	Piezoelectric voltage and current enhanced by 5.2 times and 6 times, respectively, as compared with bulk PVDF film nanogenerators under the same sonic input.
Jahan et al. (2019) <sup>[95]</sup>	PVDF	251, 327	–	–	–	Excellent thermal stability.
Zhukov et al. (2020) <sup>[96]</sup>	PLA	600	44	–	–	After 20 days of being poled, the piezoresponse decreased to half of its first value, but after long time it became constant.

and higher piezoelectric constant ( $d_{33}$ ), making them the most important materials in modern electronics applications.

### 3.2.1. Polyolefin-Based Cellular Piezoelectric Composites

**PP-Based Cellular Piezoelectric Composites:** The PP filled with organic and/or inorganic additives to increase charge storage stability was also studied. The low-compatibility fillers in the matrix should be used to assist the creation of gaps during film stretching. PP–CaCO<sub>3</sub> was reported as the most used polymer composite for cellular ferroelectrics research and the prism-shaped CaCO<sub>3</sub> was noted as a more suitable filler for stress concentrations and hence crack initiation.<sup>[15]</sup>

In 2006, Behrendt et al.<sup>[97]</sup> reported i-PP piezoelectrets filled with NA11 (2, 2'-methylene-bis-(4, 6-di-tert-butylphenyl)-phosphate) particles and hollow glass spheres. An enhancement in the stability of charge storage was noted for cellular electrets due to the formation of cavities, which were responsible for slowing down the charge drift through the film volume. Moreover, the hollow glass sphere-filled cellular stretched sample was made to be piezoelectric via the corona poling process. Films were medium stretched (draw ratios 3.5: 3.5) and highly stretched (draw ratios of 5:5) and a direct influence of this on the cavity formations in the sample and hence piezoelectricity was noted. The highly stretched i-PP films with 10 wt% of NA11 showed excellent electret features and were recognized as nucleating agent additives for i-PP. In addition,  $d_{33}$  of 179 pC N<sup>-1</sup> was measured in these films. The sample with i-PP films with glass spheres showed  $d_{33}$  between 17 and 170 pC N<sup>-1</sup> and it was dependent on glass concentration, size, and draw ratio.

Gilbert-Tremblay et al.<sup>[98]</sup> investigated the effect of particle size (0.7, 3.2, and 12 μm), the pressure, and the particle concentration (5–20 wt%) on the cellular structured piezoelectric PP–CaCO<sub>3</sub> films. The twin-screw extrusion was used to stretch the films and form cells around the filler particles. They reported an

increase in the sample's crystallinity with filler content for low filler loading. However, at higher loading, crystallinity reduced because the fillers' agglomeration prevented the polymer chain mobility. Also, during the stretching step, the smallest-sized filler incapable of creating cells, and particles with 3 μm size, started to propagate cracks around the particles in the sample.

Klimiec et al.<sup>[99]</sup> presented a method to prepare cellular PP electrets via the introduction of 5% mineral filler (a mixture of crystalline silica, kaolin, and colloidal silica) to isotactic-polypropylene(i-PP). Then, the film stretched to form a composite cellular structure. Afterward, electrets were generated by film polarization using a constant electric field from 100 to 125 V μm<sup>-1</sup> and heated up to 80 °C in a climatic chamber. The depolarization temperature (maximum density of the discharge current noted) for cellular film electrets was found to be 108 °C and the activation energy was ≈6.25 eV. The piezoconstant  $d_{33}$  was noted as 135 and 60 pC N<sup>-1</sup> for the stress of 1–120 kPa, respectively, which was three times higher as compared with the atactic phase of the PP film and PVDF film with no cellular structure.

Recently, Kaczmarek et al.<sup>[100]</sup> prepared a commercial silicate-modified PP composite by extrusion and the composites were then electrically polarized. They investigated the filler content effect on the structural and physicochemical properties of the sample. They found that growth in the filler content in the film resulted in enhanced film porosity, the Young's modulus, and crystallinity degree reached 70% of the sample with 10% of the filler. A  $d_{33}$  of ≈200 pC N<sup>-1</sup> and improved thermal stability of the sample were also noted.

**PE-Based Cellular Piezoelectric Composites:** Recently in 2019, Kaczmarek et al.<sup>[101]</sup> studied the influence of glass beads (GB)-shaped SiO<sub>2</sub> filler on PE composite. They prepared two kinds of composites, the nonoriented and oriented one via extrusion followed by uniaxial stretching and direct-current charging (100 V μm<sup>-1</sup>) at 85 °C. **Figure 12-ia,b** shows the

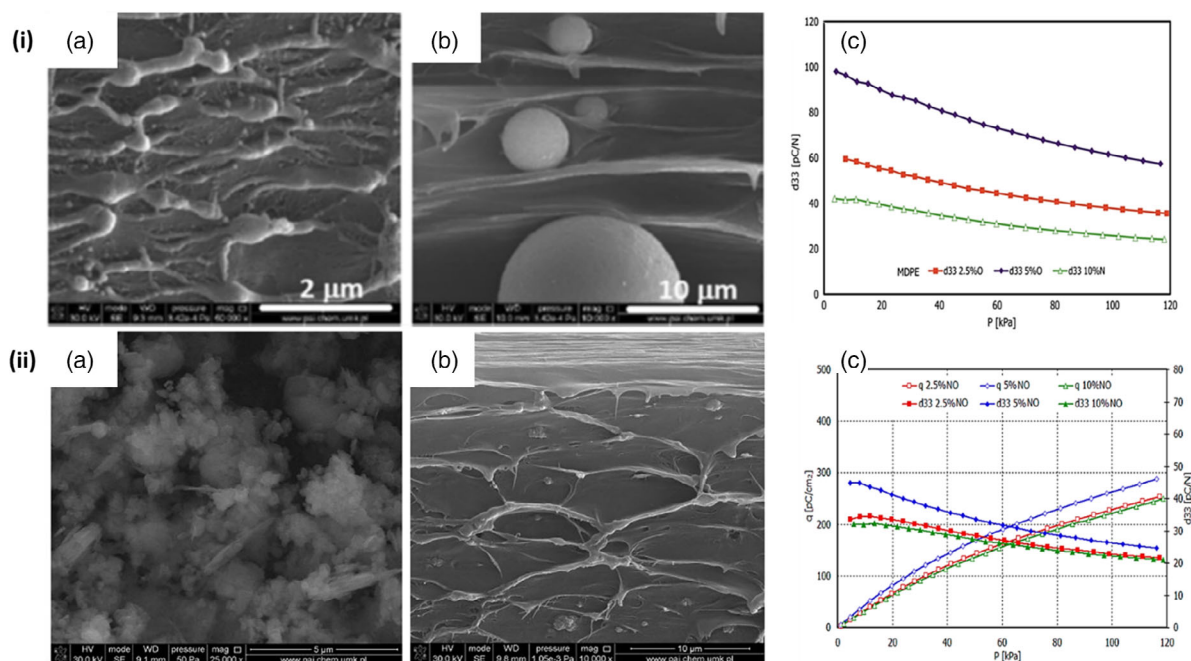


**Figure 12.** i) GB-filled PE. a,b) SEM images of oriented MDPE + 2.5% and MDPE + 10% sample, respectively. c) Plot between piezoelectric coefficients ( $d_{33}$ ) and stress for the oriented and nonoriented HDPE composites with 2.5, 5, and 10% GB. Reproduced with permission.<sup>[101]</sup> Copyright 2019, Springer Nature. ii) Aluminosilicate-filled MDPE piezoelectret. a) SEM image of MDPE + 5% sillikolloid P87 nonoriented sample. b) SEM image of its cross section. c) Plot among  $g_{33}$ ,  $d_{33}$ , and mechanical stress for nonoriented films HDPE + Sillikolloid P87. Reproduced with permission.<sup>[102]</sup> Copyright 2019, MDPI.

morphology-oriented MDPE + 2.5% and MDPE + 10% sample. The maximum value  $d_{33}$  of  $\approx 100 \text{ pC N}^{-1}$  was noted for 5% of GB-filled oriented MDPE under lower stresses of  $\approx 10 \text{ kPa cm}^{-2}$  and  $d_{33}$  of  $\approx 60 \text{ pC N}^{-1}$  was found for higher stresses of  $\approx 120 \text{ kPa cm}^{-2}$  (Figure 12-ic) and the coefficient  $g_{33}$  was found ranging from 4 to  $8 \text{ Vm N}^{-1}$ . They also tested the stability of stored electrets for 2–5 months. In another study, Kaczmarek et al.<sup>[102]</sup> used the previous method and produced two HDPE- and MDPE-based piezoelectret composite films with aluminosilicate as fillers (SEM images in Figure 12-ii,a,b. The non-oriented samples of both PE types showed the greatest value of  $d_{33}$  for 5 wt% filler contents; it attained from  $\approx 47$  to  $\approx 23 \text{ pC N}^{-1}$  for smaller stresses and from  $\approx 35$  to  $\approx 20 \text{ pC N}^{-1}$  for greater stresses. The highest value of  $d_{33}$  was noted for 10% sillikolloid-filled oriented HDPE(P87) and  $d_{33}$  of  $\approx 65 \text{ pC N}^{-1}$  for smaller stresses and  $42 \text{ pC N}^{-1}$  for higher stresses were achieved, as shown in Figure 12-ii,c.  $d_{33}$  for P87 films was considerably less and the highest values were from  $\approx 25$  to  $\approx 18 \text{ pC N}^{-1}$  for films with 5 wt% filler content in the matrix (Table 6).

### 3.2.2. PVDF-Based Cellular Piezoelectric Composites

PVDF and their related copolymers can contribute an extra functionality to a piezoelectret, because of its intrinsic polar C—F bonds and the possibility of spontaneous production of electroactive  $\beta$ - or  $\gamma$ -crystal phases. The creation and orientation of polar crystallites can be influenced further by foaming or the insertion of nanoparticles, which result in the self-poling effect, and hence

the use of physical stretching or electrical poling procedures is no longer necessary.

Ghosh et al.<sup>[30,103]</sup> used the above technique and realized a simple, cheap, and scalable porous and flexible polymer composite membrane nanogenerator (PPCNG)-based wireless green EH to power up smart electronic gadgets based without poling. They achieved this using the self-polarized platinum (Pt) nanoparticles-doped porous PVDF–HFP poly(vinylidene fluoride-co-hexafluoropropylene) membrane. The preparation method was a three-step procedure, as shown in Figure 13a. Step I involved the formation of  $\approx 150 \mu\text{m}$ -thick films via the solution casting method (Figure 13a-i). In step II, silver paint was used to make electrode skin on both sides of the film sample and then metallic wires were contacted using silver paste, which was finally dried at  $60^\circ\text{C}$  (Figure 13a-ii). Step III comprised encapsulation with PDMS and curing (Figure 13a-iii).

In one study,<sup>[103]</sup> they demonstrated a high  $d_{33}$  coefficient of  $\approx 686$  with superior remnant polarization ( $P_r$ ) of  $\approx 61.7 \mu\text{C cm}^{-2}$  and huge dielectric features such as  $\epsilon_r = 2678$  and  $\tan\delta = 0.79$  at 1 kHz. They produced a new kind of ferroelectrets nanogenerator (FTNG) with an open-circuit voltage (18 V) and short-circuit current ( $17.7 \mu\text{A}$ ) generated under 4 MPa stress. They showed FTNG capability through self-powering 25 green LEDs, 50 blue LEDs, and many capacitors with a high piezoconversion efficiency of  $\approx 0.2\%$ . In another similar study,<sup>[30]</sup> angular near-edge X-Ray absorption spectroscopy was used to realize the  $-\text{CH}_2/-\text{CF}_2$  dipole orientations caused by self-polarization. A high  $d_{33}$  coefficient of  $\approx 836 \text{ pC N}^{-1}$  and  $g_{33}$  coefficient of  $\approx -0.035 \text{ Vm N}^{-1}$  with huge remnant polarization ( $P_r$ ) of  $68 \mu\text{C cm}^{-2}$  were noted.



**Table 6.** Summary of various polyolefin-based cellular piezoelectric composites.

Author	Polymer	Filler	$d_{33}$ [ $\text{pC N}^{-1}$ ]	$g_{33}$ [ $\text{Vm N}^{-1}$ ]	Output power	Highlights
Behrendt et al. (2006) <sup>[97]</sup>	PP	,2'-methylene-bis-(4,6-di-tert-butylphenyl)-phosphate particles hollow glass spheres	179 17–170	–	–	–
Gilbert-Tremblay et al. (2012) <sup>[98]</sup>	PP	CaCO <sub>3</sub>	–	–	–	Fabricated via twin-screw extrusion.
Klimiec et al. (2015) <sup>[99]</sup>	PP	Mix of Silica, Caoline	135–60	–	–	–
Kaczmarek et al. (2017) <sup>[100]</sup>	PP	Commercial silicate	200	–	–	Fabricated via extrusion; an improved thermal stability of sample was noted.
Kaczmarek et al. (2019) <sup>[101]</sup>	o-MDPE	GB	100, 60	4-8	–	–
Kaczmarek et al. (2019) <sup>[102]</sup>	o-HDPE no-HDPE & no-MDPE	Aluminosilicate	60 47–23 under lower stresses 35–20 under higher stresses	–	–	–

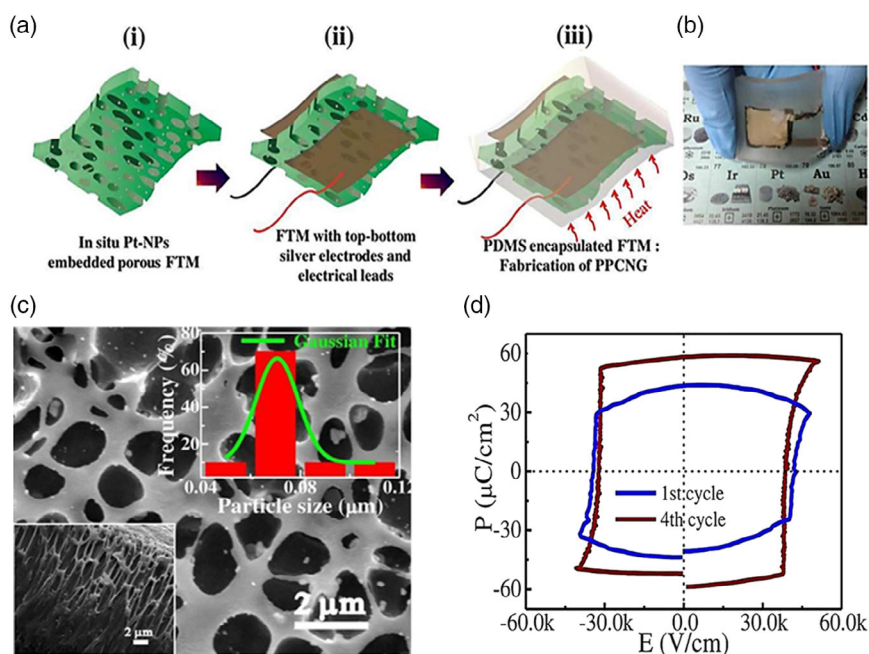


**Figure 13.** a) Illustration of PPCNG fabrication procedure: i) in situ Pt NPs-embedded porous FTM is shown, ii) the top and bottom silver electrode printing process and connection of two electrical leads, and iii) the PDMS encapsulating process. b) The digital photograph of PPCNG showing the flexibility by human fingers. c) SEM image with zoomed-in view of the selected top surface and the histogram showing Pt NP size distribution. d) Polarization–electric field loop of porous P(VDF–HFP)-based composite. Reproduced with permission.<sup>[30]</sup> Copyright 2016, AIP Publishing.

Also, a high electrical open-circuit throughput such as open-circuit voltage (from 2.7 to 23 V) and short-circuit current (from 2.9 to 24.7  $\mu\text{A}$ ) under the stress was made using a periodic motion of the human finger. They showed a wireless transfer of harvested electrical energy by visible and IR transmitter–receiver systems with a power efficiency of 17% and 49%, respectively. Further, Ghosh et al.<sup>[104]</sup> fabricated a composite film of ytterbium ( $\text{Yb}^{3+}$ ) and porous PVDF-based flexible FTNG without

any conventional poling treatment. Again, self-polarized dipoles  $\text{CH}_2/\text{CF}_2$  and porous structures contributed to the extraordinary piezo-output and dielectric properties, making it capable of capturing many forms of abundant mechanical energy sources such as movement of human finger, sound waves, and machine vibrations. They reported a piezocoefficient of  $d_{33} \approx 362.9 \text{ pC N}^{-1}$  and found it capable of powering up several electronic devices instantly. In 2017, Mahanty et al.<sup>[105]</sup> followed the same process

**Table 7.** Summary of various PVDF-based cellular piezoelectric composites.

Author	Polymer	Filler	$d_{33}$ [pC N <sup>-1</sup> ]	$g_{33}$ [Vm N <sup>-1</sup> ]	Output power	Highlights
Ghosh et al. (2015) <sup>[103]</sup>	PVDF–HFP	Platinum (Pt) nanoparticles	686	–	–	FTNGs were capable of self-powering 25 green LEDs, 50 blue LEDs, and many capacitors with a high piezoconversion efficiency of ≈0.2%.
Ghosh et al. (2016) <sup>[30]</sup>	PVDF–HFP	Platinum (Pt) nanoparticles	836	–0.035	–	A high open-circuit throughput: open-circuit voltage (from 2.7 to 23 V) and short-circuit current (from 2.9 to 24.7 μA) under the periodic human finger stress.
Ghosh et al. (2016) <sup>[104]</sup>	PVDF	Ytterbium (Yb3+)	362.9	–	–	Self-poled FTNG.
Mahanty et al. (2017) <sup>[105]</sup>	PVDF–HFP	ZnO nanoparticles	–	–0.076	–	An open-circuit voltage (9 V) and short-circuit current (1.3 mA cm <sup>-2</sup> ) generated under cyclic mechanical stress of 0.36 MPa.
Rahimabady et al. (2017) <sup>[106]</sup>	PVDF	SWCNTs	–	–	–	A sound absorption coefficient greater than 50% at 600 Hz was noted.
Jahan et al. (2018) <sup>[107]</sup>	PVDF	Montmorillonite (MMT)–CaCO <sub>3</sub>	137–251	–	–	–
Xu et al. (2020) <sup>[108]</sup>	PVDF	MWCNTs	–	–	–	An output of 6.5 V when imposed to harmonic compression, able to lighten four LEDs.

and prepared porous membrane ZnO NPs-filled P(VDF–HFP) films containing ferroelectric phases of ≈88%, with a high  $d_{33}$  of ≈–15.2 pC N<sup>-1</sup> and  $g_{33}$  ≈ of –0.076 Vm N<sup>-1</sup>. They showed that the flexible nanogenerator generates an open-circuit voltage (9 V) and short-circuit current (1.3 mA cm<sup>-2</sup>) under cyclic mechanical stress of 0.36 MPa.

Rahimabady et al.<sup>[106]</sup> demonstrated a composite foam fabricated from porous polar PVDF mixed with the conductive single-walled carbon nanotube (SWCNTs) to boost airborne sound absorption. They obtained the sound absorption coefficient greater than 50% at 600 Hz with a sound reduction coefficient higher than 0.58 with the composition of PVDF/5 wt% SWCNT.

Recently, Jahan et al.<sup>[107]</sup> produced cellular PVDF–montmorillonite (MMT)–CaCO<sub>3</sub>-based piezoelectret films involving uniaxially stretched, GDE treated, and corona charged. Recently, Jahan et al.<sup>[107]</sup> produced cellular PVDF–montmorillonite (MMT)–CaCO<sub>3</sub>-based piezoelectret films involving uniaxial stretching, GDE treatment, and corona charging. Also, they showed that the highest  $d_{33}$  (from 137 to 251 pC N<sup>-1</sup>) was generated when there was increase in the inflation pressure (from 3 to 5 MPa) at 130 °C constant temperature for a certain time.<sup>[107]</sup>

More recently, Xu et al.<sup>[108]</sup> fabricated a foamed PVDF/multiwalled carbon nanotube (MWCNT) piezozanocomposite. The foam layer was created by the bead foaming technology utilizing supercritical carbon dioxide (scCO<sub>2</sub>). They reported dispersion of MWCNTs, which enhanced heterogeneous nucleation and effects due to MWCNT on PVDF, which resulted in unique and denser cellular structures and the compressive strain was ≈1.1 MPa greater than the pure foam. The squeezing and plasticizing effect of scCO<sub>2</sub> on the PVDF matrix contributed to an increase in the β-phase crystal of PVDF, thus responsible for good piezoelectricity with an output of 6.5 V when imposed to harmonic compression. The generated voltage can light four LEDs, which can have wide applications in smart electronics (Table 7).<sup>[108]</sup>

### 3.3. Molecularly Doped Piezoelectric Foams

As the name suggests, the method of generation of piezoelectricity in this type of piezof foam is based on doping a nonpolar polymer foam with highly polar molecules followed by the poling process. The molecularly doped piezofoams are new types of piezoelectric materials in which electric polarization is not generated due to the foam structure unlike in conventional space-charge electrets but simply responsible for desirable mechanical properties, and the highly polar foreign (doping) molecules are responsible for piezoelectricity phenomenon. **Figure 14** shows a schematic of the materials system and the generation of polarization and piezoelectricity.<sup>[109]</sup> When a compressive force is applied to these foams, the dipole moment density increases due to fixed guest dipoles, inducing a surface charge and hence current flow. The fabrication approach could be used for other materials having greatly low bulk moduli for example brush polymers.

#### 3.3.1. Molecularly Doped Piezoelectric Polyurethane (PU)

Moody et al. in 2016 fabricated a piezoelectric system using a process called “doped nonpolar polymers.” They used highly polar dopant moieties such as 2-chloro-4-nitroaniline (CNA) into the flexible nonpolar polyurethane (PU) foam (polymer matrix) to enhance their piezooutputs multiple times higher than traditional piezoelectric ceramics or polymers. They measured massive piezoelectric coefficients  $d_{33}$  around 244 ± 30 pC N<sup>-1</sup> at 400 Vm m<sup>-1</sup> poling field. They also showed better current and voltage output response corresponding to very low applied pressure imparted by the human body movement. For example, they demonstrated the output power of a sample with a piezoelectric coefficient of 112 pC N<sup>-1</sup> using typical finger taps and yielded a peak current output of 5 nA and peak power of

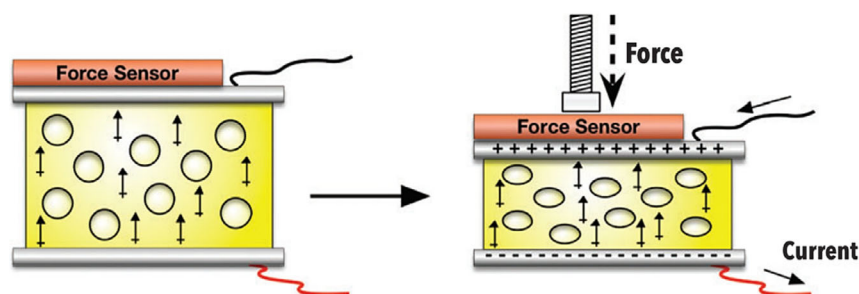


**Figure 14.** Schematic of the material, in which compression of foam causes an increase in dipole moment density due to fixed guest dipoles, inducing surface charge and current flow.<sup>[10]</sup> Reproduced with permission.<sup>[10]</sup> Copyright 2016, The Royal Society of Chemistry.

5 nW, with the power output varying with tapping intensity. **Figure 15a** shows power versus time, and **Figure 15b** shows the device, emphasizing high flexibility. Further, the observed piezocoefficient  $d_{33}$  increased with poling field, as shown in **Figure 15c**.<sup>[10]</sup>

### 3.3.2. Molecularly Doped Piezoelectric Polydimethyl Siloxane (PDMS)

Recently, Petroff et al.<sup>[110]</sup> reported a high piezoelectric response of  $153 \text{ pC N}^{-1}$  in polar molecule-doped PDMS foam. They used the same design concept reported by Moody et al.<sup>[10]</sup> except that they used a sugar template for producing PDMS foam. They doped polydimethylsiloxane (PDMS) foam with eight different highly polar small organic molecules such as 2-chloro-4-nitroaniline (CNA) and 4-nitro-1,2-phenylenediamine, 2-methyl-4-nitroaniline (MNA), 3-aminobenzoic acid, N, N-dimethyl-4-nitroaniline, 4-nitro acetanilide, acetanilide, benzoic acid, acetonitrile and, 1,4-dibromobenzene as shown in **Figure 16b** with varying amounts of and electrically poling at various voltages. **Figure 16a** shows a graph of piezoelectric response as a function of dopant dipole moment for samples

poled at  $200 \text{ Vm}^{-1}$  after being doped with a 0:1 m solution (**Table 8**).<sup>[110]</sup>

### 3.4. Solid Polyelectrolyte-Filled Cellular Piezoelectric Polymer

Piezoelectricity in this novel solid polyelectrolyte-filled cellular polymer is attributed due to the strong action of intrinsic polarity and orientation of molecular dipoles of polymer (e.g., PVDF) cells, formed when pressure crystallized, with artificial macroscopic solid electrolyte (Nafion) dipole fillers on several micrometers scale, generated via their internal ionic mobility during the deformation of the cell wall.

Xu et al.<sup>[29]</sup> reported a novel polymeric piezoelectret generator without any poling requirement developed utilizing new techniques of design and fabrication, which showed an outstanding property for dynamic energy harvesting (**Figure 17c,d**). The reported piezoelectret was a cellular piezopolymer filled with a solid polyelectrolyte. In their study, they fabricated a PVDF–Nafion composite via solution casting following high-pressure crystallization (**Figure 17a**). High pressure and compositional variation in PVDF–Nafion showed control of sample cells size and morphology as well as their substructures and crystalline

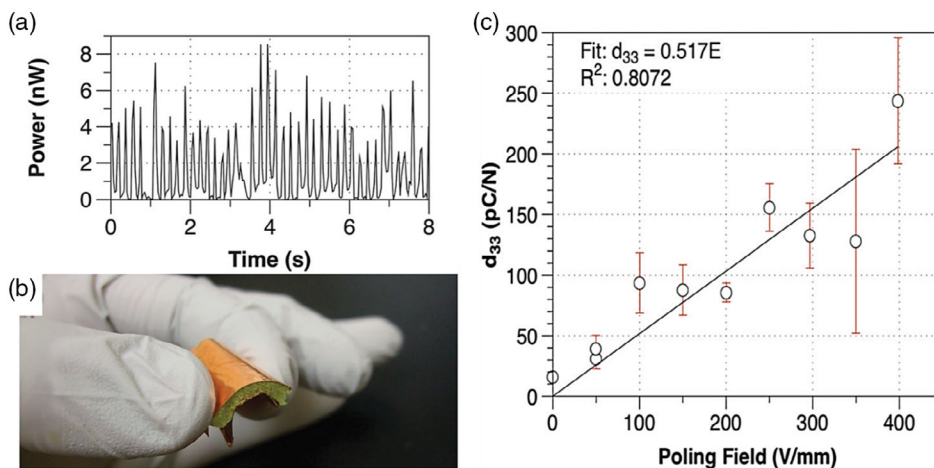


**Figure 15.** a) Power dissipated in the load versus time for a sample subjected to light finger taps, with an average power of 1.5 nW. b) The piezomaterial is extremely flexible and flexional motion also generates electric charge. c) Graph between piezoelectric coefficient ( $d_{33}$ ) and poling electric field for PU foam sample doped with 0.2 M CNA (2-chloro-4-nitroaniline). Reproduced with permission.<sup>[10]</sup> Copyright 2016, The Royal Society of Chemistry.

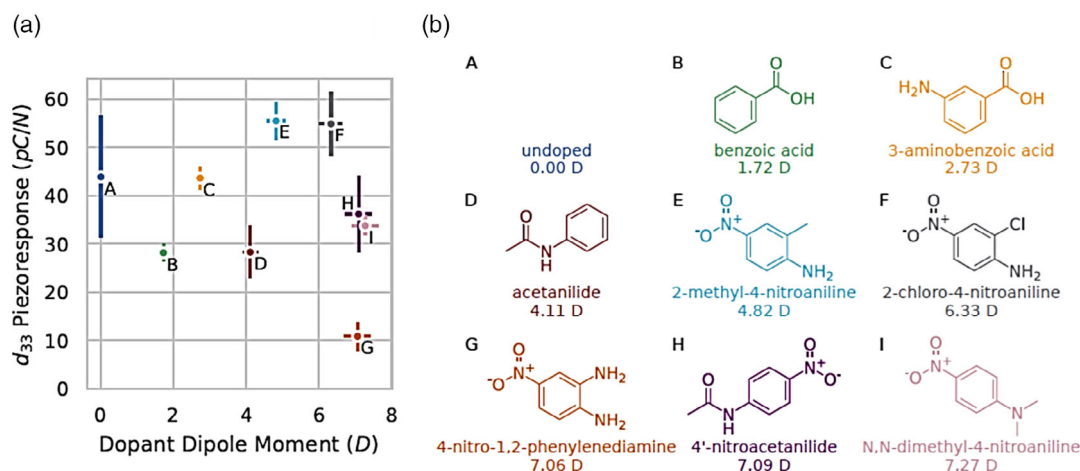


**Figure 16.** a) Piezoelectric response as a function of the dopant dipole moment for samples poled at  $200 \text{ V mm}^{-1}$  after being doped with 0:1 m solution. X-axis error bars are 5%; Y-axis error bars represent standard error across at least four samples. b) Different highly polar small organic molecules. Reproduced with permission.<sup>[110]</sup> Copyright 2019, American Chemical Society.

**Table 8.** Summary of molecularly doped piezoelectric foam.

Author	Polymer	Dopant	$d_{33}$ [pC N <sup>-1</sup> ]	$g_{33}$ [Vm N <sup>-1</sup> ]	Output power	Highlights
Moody et al. (2016) <sup>[10]</sup>	PU	2-chloro-4-nitroaniline (CNA)	244	–	≈5 nW	A better $V-I$ output response with a low applied pressure for example human finger touch.
Petroff et al. (2019) <sup>[110]</sup>	PDMS	2-Chloro-4-nitroaniline (CNA) 4-nitro-1,2-phenylenediamine 2-Methyl-4-nitroaniline (MNA), 3-aminobenzoic acid N, N-Dimethyl-4-nitroaniline, 4-nitroacetanilide, acetanilide, Benzoic acid, Acetonitrile, 1,4-dibromobenzene.	153	–	–	–

forms (Figure 17b). The output open-circuit voltage density of the generator was found as  $14.6 \text{ V cm}^{-2}$  at optimized conditions and when stimulated under dynamic deformation, exceeded the most polymer-based piezoelectric systems in previous literature. Also, the generator showed nice durability and stability, and the non-decayed electrical output was observed for more than 100 000 continuous cycles of functioning. This was also reported that the facile fabrication of these unique electret materials and their applications in PEHs may lead to a new paradigm of piezoelectrets. Further in 2018, Xu et al.<sup>[111]</sup> improved the (mechanical–electrical) conversion efficiency of the self-poled PVDF/Nafion through the introduction of graphene-quantum-dots (GQDs) into the matrix. The nanogenerators were stimulated by a 60 N applied force at a 5 Hz frequency. The generated output SC currents of 50, 20, and 60 nA and output OC voltages were measured for GQD loading of 0, 1, and 3, respectively. These values were much improved for NaCl-soaked nanogenerators with output SC currents of 60, 60, and 85 nA and output OC voltages of 3.9, 3.3, and 5.0 V for the same GQD loading, respectively. They achieved ≈20% enhancement in output SC current

and ≈25% enhancement in output OC voltage for nanogenerators based on PVDF/Nafion/GQDs as compared with its PVDF/Nafion-based counterpart. It was found that this improvement was due to the GQDs (Table 9).

## 4. Applications

Polymeric foam-based piezoelectrics have a broad range of technological applications in a variety of fields, such as energy harvesting, sensing, and actuation devices and systems.<sup>[112]</sup> These piezo-based devices and systems are now revolutionizing the technological market trend due to their greater accuracy, lower costs, higher reliability, and multifunctionality.<sup>[113]</sup>

One of the major application areas includes the biomedical sector where flexible polymers are used as potential materials for artificial muscle actuators, explored as intrusive medical robots for diagnosis and microsurgery, and used as actuator implants for stimulating the growth of bones and tissues, thanks to their property of high impedance matching toward the human

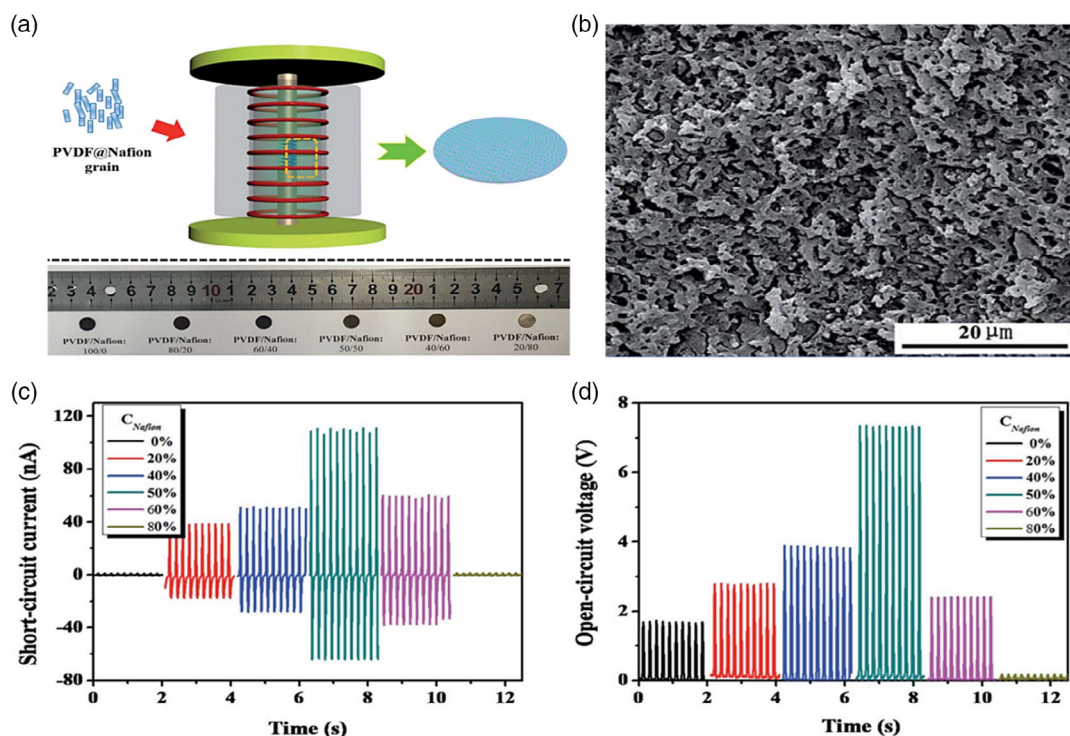


**Figure 17.** a) Schematic diagram showing the fabrication process of the PVDF–Nafion dynamic piezoelectrets (PNDP) with a piston–cylinder high-pressure apparatus and a digital picture showing the physical size and appearance of the as-fabricated PNDP samples. b) Cross-sectional view of the SEM images of the PVDF–Nafion composite samples with compounding ratios of PVDF/Nafion:50/50, wt./wt., crystallized at 400 MPa, at 260 °C for 10 min. c) Short-circuit current of the PNDPGs, and d) the corresponding open-circuit voltage, generated at a stimulated frequency of 5 Hz and applied force of 60 N. Reproduced with permission.<sup>[29]</sup> Copyright 2017, The Royal Society of Chemistry.

**Table 9.** Summary of solid electrolyte-filled piezoelectric foam.

Author	Polymer	Electrolyte	Fillers	Output parameters	Highlights
Xu et al. (2017) <sup>[29]</sup>	PVDF	Solid Nafion	–	Output voltage density: $\approx 14.6 \text{ V cm}^{-2}$	A novel fabrication method of self-poled polymeric piezoelectric energy generator.
Xu et al. (2018) <sup>[111]</sup>	PVDF	Solid Nafion	GQDs	–	Self-poled nanogenerator. They achieved an enhancement of $\approx 20\%$ in output SC current and $\approx 25\%$ in output OC voltage for PVDF/Nafion/GQDs-based nanogenerators as compared with its PVDF/Nafion-based counterpart.

body fluids, tissues, and other portable devices which makes them an ideal candidate for such applications.<sup>[18,114–125]</sup> However, apart from the biomedical sectors, broad applications of polymeric PEH systems are found in the wireless network sensor,<sup>[126–134]</sup> optics, robotics, environmental monitoring,<sup>[135]</sup> underwater and electroacoustic transducers,<sup>[136]</sup> ultrasonics acoustic devices,<sup>[137]</sup> piezoelectric roads,<sup>[138]</sup> etc.

Moreover, today, scientists and engineers are working on the fabrication and development of PEH systems based on the movement of the human body or muscles, which includes electroartificial skin, human health monitoring patch, e-textiles, piezoshoe, piezoelectric-based dancing floor, etc.<sup>[139–155]</sup> These are based on human body activities such as running, walking, dancing, and breathing, which create vibrations and ultimately

generate power to power miniature electronic systems and devices. The production of piezoelectric systems from lightweight polymeric foam-based systems has become crucial and is gaining commercial importance. The applications of PEHs in different fields based on natural and artificial mechanical energy sources are shown in **Figure 18a,b**.

## 5. Future Perspectives of PEHs

In the modern age, piezoelectric materials systems and devices are considered to increase, being the most significant usable materials for energy to minimize the excess consumption of conventional fossil energy and renewable energy-harvesting

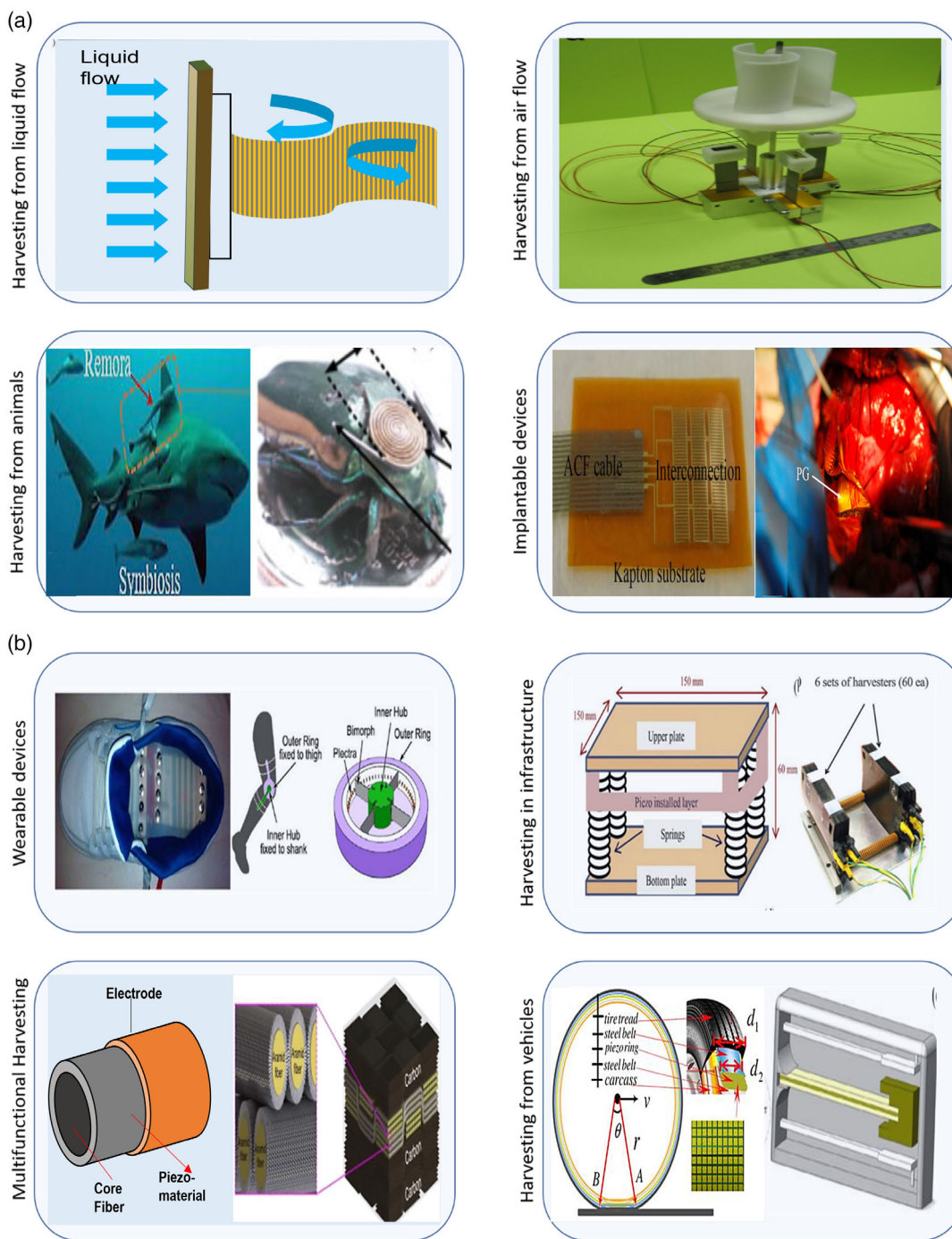


**Figure 18.** Application of PEHs in different fields. a) Harvesting from liquid flow. Harvesting from air flow. Reproduced with permission.<sup>[141]</sup> Copyright 2013, Elsevier. Harvesting from animals. Reproduced with permission.<sup>[142]</sup> Copyright 2022, Elsevier. Reproduced with permission.<sup>[143]</sup> Copyright 2011, IOP Publishing Ltd., Implantable devices. Reproduced with permission.<sup>[145]</sup> Copyright 2015, Elsevier. b) Wearable devices. Reproduced with permission.<sup>[146]</sup> Copyright 2014, MDPI. Reproduced with permission.<sup>[147]</sup> Copyright 2012, IOP Publishing Ltd. Harvesting in infrastructure. Reproduced with permission.<sup>[148]</sup> Copyright 2015, Elsevier. Reproduced with permission.<sup>[149]</sup> Copyright 2017, Elsevier. Multifunctional harvesting. Reproduced with permission.<sup>[151]</sup> Copyright 2016, The Royal Society of Chemistry. Harvesting from vehicles. Reproduced with permission.<sup>[152]</sup> Copyright 2015, Elsevier. Reproduced with permission.<sup>[153]</sup> Copyright 2012, Elsevier.

sources.<sup>[156]</sup> In addition to zero-carbon dioxide emissions and aggressive power systems, these materials have been

distinguished by improved functionality for power generation from unnecessary physical vibration sources.

These materials systems are able to produce cleaner energy, along with significant portability and considerable time savings. In contrast, the commercialization and market development of polymer PEHs are highly contingent on two key factors, improving the energy performance of the associated systems and devices in line with the specifications and reducing prices, to cope with traditional piezoceramics.

Some essential considerations also include the design and manufacture of systems, good lifetime and fulfillment of the performance parameter, and compliance with modern technologies.

Researchers expect that PEH will be taking 28.8% of the entire energy collection market very soon, due to the rising number of environmentally sustainable piezoelectric projects.<sup>[157]</sup>

This will surely revolutionize the energy harvest output while integrating creativity with technology to form next-generation energy. PEH has become an important research area by going forward through the continuous development and progression of low-power electronics. Today, high-end PEH harvesters produce total energy up to significant mW. It is expected that in 2025, PEHs will expand internationally and reach in excess of 800 million dollars, indicating a strong trend.<sup>[156]</sup>

## 6. Conclusion

One of the most important classes of functional materials is the polymeric foam-based piezoelectric that can be used for various energy-harvesting applications. It has been an incredibly wide area of research over the past 20 years. While it is impossible to summarize all the works conducted in this field in the last decade, this article aims to provide a succinct overview of the most powerful studies published in the field of polymeric foam-type piezoelectric materials. Based on our review results of various polymer-based piezoelectrets, several concluding remarks can be drawn as follows: 1) The main methods used for the production of conventional single- or multiple-layered cellular polymeric piezoelectrets are generally produced by stretching and foaming; 2) The fluoropolymer-based multiple layers, for example, two-layered FEP (one wavy layer negative corona charged and other uncharged), are comparable with the best bipolar EHs, while the AF-based single-layer piezoelectret gives great charge storage capability and hence higher voltage output; 3) In the group of cellular piezoelectric composites, Pt nanoparticles/ PVDF-HFP composite has the highest  $d_{33}$  coefficient and can be utilized for PEHs; 4) The molecularly doped piezoelectric foam such as CNA-doped PU is extremely sensitive to pressure even with a low applied pressure, for example, human finger touch, and hence can be used in making highly sensitive implantable devices. In these systems, unlike in conventional space-charge electrets, highly polar foreign (doping) molecules are responsible for piezoelectricity phenomena, while foaming structures only provide mechanical properties; 5) In the case of novel solid polyelectrolyte-filled cellular piezoelectrets, for example, PVDF/Nafion, self-poled piezoelectrets in which piezoelectricity is attributed to the strong action of intrinsic polarity and orientation of molecular dipoles of polymer. A significant enhancement in output current and output voltage is noted for PVDF/Nafion/GQDs-based nanogenerators as compared with its PVDF/Nafion-based counterpart; and 6) The facile

fabrication of these unique and novel piezoelectret materials and their applications in PEHs may lead to a new paradigm of piezoelectrets.

These special piezoelectric materials can be utilized for PEH devices and systems as a strong substitute for conventional piezoceramics or piezopolymers. This technology may also be the revolutionary by eliminating piezoceramics entirely due to its compact and convenient attributes. These piezoelectric systems have flexibility, adaptability, easy manufacturing, and accessibility over conventional systems and can power uninterrupted-power to low-power electronics. The research on polymeric piezoelectret foam materials would undoubtedly continue, and many new applications based on all these new electret materials are envisaged in the near future.

## Acknowledgements

The author is thankful to the Hevesy György PhD School of Chemistry, Eötvös Loránd University, Hungary, for valuable scientific and technical support.

## Conflict of Interest

The authors declare no conflict of interest.

## Keywords

energy harvesting, fabrications, foams, piezoelectricity, polymers

Received: May 5, 2022

Revised: May 29, 2022

Published online:

- [1] S. Mishra, L. Unnikrishnan, S. K. Nayak, S. Mohanty, *Macromol. Mater. Eng.* **2019**, *304*, 1800463.
- [2] M. Safaei, H. A. Sodano, S. R. Anton, *Smart Mater. Struct.* **2019**, *28*, 113001.
- [3] S. Trolrier-Mckinstry, S. Zhang, A. J. Bell, X. Tan, *Annu. Rev. Mater. Res.* **2018**, *48*, 191.
- [4] C.-T. Pan, C.-K. Yen, H.-C. Wu, L. Lin, Y.-S. Lu, J. C.-C. Huang, S.-W. Kuo, *J. Mater. Chem. A* **2015**, *3*, 6835.
- [5] S. Harstad, N. D'Souza, N. Soin, A. A. El-Gendy, S. Gupta, V. K. Pecharsky, T. Shah, E. Siores, R. L. Hadimani, *AIP Adv.* **2017**, *7*, 056411.
- [6] F. Wang, Y.-W. Mai, D. Wang, R. Ding, W. Shi, *Sens. Actuators, A* **2015**, *233*, 195.
- [7] Y. Qi, N. T. Jafferis, L. Kenneth Jr, C. M. Lee, H. Ahmad, M. C. Mcalpine, *Nano Lett.* **2010**, *10*, 524.
- [8] H. Kaczmarek, B. Królikowski, E. Klimiec, M. Chylińska, D. Bajer, *Russ. Chem. Rev.* **2019**, *88*, 749.
- [9] X. Quan, C. W. Marvin, L. Seebald, G. R. Hutchison, *J. Phys. Chem. C* **2013**, *117*, 16783.
- [10] M. J. Moody, C. W. Marvin, G. R. Hutchison, *J. Mater. Chem. C* **2016**, *4*, 4387.
- [11] R. Gerhard-Multhaupt, *IEEE Trans. Dielectr. Electr. Insul.* **2002**, *9*, 850.
- [12] K. S. Challagulla, T. A. Venkatesh, *Acta Mater.* **2012**, *60*, 2111.
- [13] A. Savolainen, K. Kirjavainen, *J. Macromol. Sci. Part B Chem.* **1989**, *26*, 583.

- [14] A. Qaiss, H. Saidi, O. Fassi-Fehri, M. Bousmina, *Polym. Eng. Sci.* **2012**, *52*, 2637.
- [15] A. Mohebbi, F. Mighri, A. Ajji, D. Rodrigue, *Adv. Polym. Technol.* **2018**, *37*, 468.
- [16] K. Sappati, S. Bhadra, *Sensors* **2018**, *18*, 3605.
- [17] Y. Zhang, C. R. Bowen, S. K. Ghosh, D. Mandal, H. Khanbareh, M. Arafa, C. Wan, *Nano Energy* **2019**, *57*, 118.
- [18] R. A. Surmenev, T. Orlova, R. V. Chernozem, A. A. Ivanova, A. Bartasyste, S. Mathur, M. A. Surmeneva, *Nano Energy* **2019**, *62*, 475.
- [19] R. A. Surmenev, R. V. Chernozem, I. O. Pariy, M. A. Surmeneva, *Nano Energy* **2021**, *79*, 105442.
- [20] J. Rödel, J.-F. Li, *MRS Bull.* **2018**, *43*, 576.
- [21] Fawad, M. J. Khan, M. A. Riaz, H. Shahid, M. S. Khan, Y. Amin, J. Loo, H. Tenhunen, *IEEE Access* **2019**, *7*, 66668.
- [22] R. Calì, U. Rongala, D. Camboni, M. Milazzo, C. Stefanini, G. De Petris, C. Oddo, *Sensors* **2014**, *14*, 4755.
- [23] P. Dineva, D. Gross, R. Müller, T. Rangelov, *Dynamic Fracture of Piezoelectric Materials*, Springer, Cham **2014**, pp. 7–32.
- [24] R. Ahmed, F. Mir, S. Banerjee, *Smart Mater. Struct.* **2017**, *26*, 085031.
- [25] Noliac, *Text. Res. J.* **2012**, *3*, 9, [http://www.noliac.com/fileadmin/user\\_upload/documents/Tutorials/Tutorials\\_Piezo\\_basics.pdf](http://www.noliac.com/fileadmin/user_upload/documents/Tutorials/Tutorials_Piezo_basics.pdf) (accessed: May 2018).
- [26] A. Toprak, O. Tigli, *Appl. Phys. Rev.* **2014**, *1*, 031104.
- [27] N. Wu, X. Cheng, Q. Zhong, J. Zhong, W. Li, B. Wang, B. Hu, J. Zhou, *Adv. Funct. Mater.* **2015**, *25*, 4788.
- [28] B. Wang, J. Zhong, Q. Zhong, N. Wu, X. Cheng, W. Li, K. Liu, L. Huang, B. Hu, J. Zhou, *Adv. Electron. Mater.* **2016**, *2*, 1500408.
- [29] C. Xu, L. Zhang, Y. Xu, Z. Yin, Q. Chen, S. Ma, H. Zhang, R. Huang, C. Zhang, L. Jin, W. Yang, J. Lu, *J. Mater. Chem. A* **2017**, *5*, 189.
- [30] S. K. Ghosh, T. K. Sinha, B. Mahanty, S. Jana, D. Mandal, *J. Appl. Phys.* **2016**, *120*, 174501.
- [31] a) X. Zhang, J. Hillenbrand, G. M. Sessler, *Appl. Phys. A* **2006**, *84*, 139; b) R. Altafim, H. Basso, R. Altafim, L. Lima, C. de Aquino, L. G. Neto, R. Gerhard-Mulhaupt, *IEEE Trans. Dielectr. Electr. Insul.* **2006**, *13*, 979.
- [32] N. Obaid, M. Kortschot, M. Sain, A. Mohebbi, F. Mighri, A. Ajji, *Polymers* **2015**, *34*, 8.
- [33] M. Wegener, *Behavior and Mechanics of Multifunctional Materials and Composites 2010*, San Diego, California, United States Vol. 7644, International Society for Optics and Photonics **2010**, p. 76441A.
- [34] S. Harris, A. Mellinger, *J. Appl. Phys.* **2014**, *115*, 163302.
- [35] X. Qiu, A. Mellinger, W. Wirges, R. Gerhard, *Appl. Phys. Lett.* **2007**, *91*, 132905.
- [36] P. Pondrom, J. Hillenbrand, G. M. Sessler, J. Bös, T. Melz, *Appl. Phys. Lett.* **2014**, *104*, 172901.
- [37] C. A. Ray, S. R. Anton, in *Active and Passive Smart Structures and Integrated Systems 2015*, Inter. Society for Optics and Photonics April **2015**, Vol. 9437, p. 943111.
- [38] M. Paajanen, M. Wegener, R. Gerhard-Mulhaupt, in *2001 Annual Report Conf. on Electrical Insulation and Dielectric Phenomena (Cat. No. 01CH37225*, IEEE, Piscataway, NJ), October **2001**, pp. 24–27.
- [39] J. Hillenbrand, X. Zhang, Y. Zhang, G. M. Sessler, in *2003 Annual Report Conf. on Electrical Insulation and Dielectric Phenomena*, IEEE, Piscataway, NJ), October **2003**, pp. 40–43.
- [40] M. Wegener, W. Wirges, R. Gerhard-Mulhaupt, M. Danschmüller, R. Schwödiauer, S. Bauer-Gogonea, S. Bauer, M. Paajanen, H. Minkkinen, J. Raukola, *Appl. Phys. Lett.* **2004**, *84*, 392.
- [41] G. S. Neugschwandtner, R. Schwödiauer, M. Vieytes, S. Bauer-Gogonea, S. Bauer, J. Hillenbrand, R. Kressmann, G. M. Sessler, M. Paajanen, J. Lekkala, *Appl. Phys. Lett.* **2000**, *77*, 3827.
- [42] X. Qiu, M. Wegener, W. Wirges, X. Zhang, J. Hillenbrand, Z. Xia, R. Gerhard-Mulhaupt, G. M. Sessler, *J. Phys. D: Appl. Phys.* **2005**, *38*, 649.
- [43] M. Sborikas, M. Wegener, *Appl. Phys. Lett.* **2013**, *103*, 252901.
- [44] S. R. Anton, K. M. Farinholt, A. Erturk, *J. Intell. Mater. Syst. Struct.* **2014**, *25*, 1681.
- [45] Z. Luo, D. Zhu, J. Shi, S. Beeby, C. Zhang, P. Proynov, B. Stark, *EEE Trans. Dielectr. Electr. Insul.* **2015**, *22*, 1360.
- [46] A. Mohebbi, F. Mighri, A. Ajji, D. Rodrigue, *Polym. Adv. Technol.* **2017**, *28*, 476.
- [47] A. Mohebbi, F. Mighri, A. Ajji, D. Rodrigue, *J. Appl. Polym. Sci.* **2017**, *134*.
- [48] A. Mohebbi, D. Rodrigue, *Polym. Eng. Sci.* **2018**, *58*, 300.
- [49] A. Samadi, R. Hasanzadeh, T. Azdast, H. Abdollahi, P. Zarrintaj, M. R. Saeb, *J. Macromol. Sci. Part B* **2020**, *59*, 376.
- [50] X. Zhang, X. Wang, J. Huang, Z. Xia, *J. Mater. Sci.* **2009**, *44*, 2459.
- [51] X. Zhang, L. Wu, G. M. Sessler, *AIP Adv.* **2015**, *5*, 077185.
- [52] G. M. Sessler, P. Pondrom, X. Zhang, *Phase Transitions* **2016**, *89*, 667.
- [53] E. C. Tefft IV, Doctoral dissertation, Tennessee Technological University **2018**.
- [54] M. Nakayama, Y. Uenaka, S. Kataoka, Y. Oda, K. Yamamoto, Y. Tajitsu, *Jpn. J. Appl. Phys.* **2009**, *48*, 09KE05.
- [55] Y. Tajitsu, *Ferroelectrics* **2011**, *415*, 57.
- [56] G. O. Braña, P. L. Segovia, F. Magraner, A. Quijano, *J. Phys. Conf. Ser.* **2011**, *301*, 012054.
- [57] D. Rychkov, R. Alberto Pisani Altafim, X. Qiu, R. Gerhard, *J. Appl. Phys.* **2012**, *111*, 124105.
- [58] H. Kaczmarek, E. Klimiec, B. Królkowski, M. Chylińska, M. Machnik, *J. Mater. Sci.: Mater. Electron.* **2017**, *28*, 16639.
- [59] O. Hamdi, F. Mighri, D. Rodrigue, *Cell. Polym.* **2018**, *37*, 153.
- [60] O. Hamdi, F. Mighri, D. Rodrigue, *Polym. Adv. Technol.* **2019**, *30*, 153.
- [61] O. Hamdi, F. Mighri, D. Rodrigue, *J. Appl. Polym. Sci.* **2019**, *136*, 47646.
- [62] M. Wegener, W. Wirges, R. Gerhard-Mulhaupt, *Adv. Eng. Mater.* **2005**, *7*, 1128.
- [63] W. Wirges, M. Wegener, O. Voronina, L. Zirkel, R. Gerhard-Mulhaupt, *Adv. Funct. Mater.* **2007**, *17*, 324.
- [64] M. Wegener, W. Wirges, J. P. Dietrich, R. Gerhard-Mulhaupt, in *2005 12th Inter. Symp. on Electrets*, IEEE, Piscataway, NJ September **2005**, pp. 28–30.
- [65] P. Fang, W. Wirges, M. Wegener, L. Zirkel, R. Gerhard, *e-Polymers* **2008**, *8*.
- [66] P. Fang, M. Wegener, W. Wirges, R. Gerhard, L. Zirkel, *Appl. Phys. Lett.* **2007**, *90*, 192908.
- [67] P. Fang, X. Qiu, W. Wirges, R. Gerhard, L. Zirkel, *IEEE Trans. Dielectr. Electr. Insul.* **2010**, *17*, 1079.
- [68] R. Gerhard-Mulhaupt, W. Kunstler, T. Gome, A. Pucher, T. Weinhold, M. Seiss, M. Zhongfu Xia, A. Wedel, R. Danz, *IEEE Trans. Dielectr. Electr. Insul.* **2000**, *7*, 480.
- [69] X. Zhang, J. Huang, Z. Xia, *Phys. Scr.* **2007**, *2007*, 274.
- [70] X. Zhang, X. Wang, G. Cao, D. Pan, Z. Xia, *Appl. Phys. A* **2009**, *97*, 859.
- [71] X. Zhang, X. Zhang, G. M. Sessler, X. Gong, *J. Phys. D: Appl. Phys.* **2013**, *47*, 015501.
- [72] H. von Seggern, S. Zhukov, S. Fedosov, *IEEE Trans. Dielectr. Electr. Insul.* **2011**, *18*, 49.
- [73] X. Zhang, G. M. Sessler, Y. Wang, *J. Appl. Phys.* **2014**, *116*, 074109.
- [74] O. Voronina, M. Wegener, W. Wirges, R. Gerhard, L. Zirkel, H. Münstedt, *Appl. Phys. A* **2008**, *90*, 615.
- [75] X. Zhang, J. Hillenbrand, G. M. Sessler, S. Haberzettl, K. Lou, *Appl. Phys. A* **2012**, *107*, 621.
- [76] B. Wang, C. Liu, Y. Xiao, J. Zhong, W. Li, Y. Cheng, B. Hu, L. Huang, J. Zhou, *Nano Energy* **2017**, *32*, 42.
- [77] X. Zhang, P. Pondrom, G. M. Sessler, X. Ma, *Nano Energy* **2018**, *50*, 52.
- [78] J. Shi, S. Yong, S. Beeby, *Smart Mater. Struct.* **2018**, *27*, 084005.
- [79] X. Ma, X. Zhang, G. M. Sessler, L. Chen, X. Yang, Y. Dai, P. He, *AIP Adv.* **2019**, *9*, 125334.



- [80] O. Ben Dali, P. Pondrom, G. M. Sessler, S. Zhukov, H. von Seggern, X. Zhang, M. Kupnik, *Appl. Phys. Lett.* **2020**, *116*, 243901.
- [81] A. Mellinger, M. Wegener, W. Wirges, R. Gerhard-Multhaupt, *Appl. Phys. Lett.* **2001**, *79*, 1852.
- [82] J. J. Wang, T. H. Hsu, C. N. Yeh, J. W. Tsai, Y. C. Su, *J. Micromech. Microeng.* **2011**, *22*, 015013.
- [83] J. J. Wang, J. W. Tsai, Y. C. Su, *J. Micromech. Microeng.* **2013**, *23*, 075009.
- [84] G. M. Sessler, G. M. Yang, W. Hatke, in *IEEE 1997 Annual Report Conference On Electrical Insulation And Dielectric Phenomena*, Vol. 2, IEEE, Piscataway, NJ, October **1997**, pp. 467–470.
- [85] M. Wegener, M. Paajanen, O. Voronina, R. Schulze, W. Wirges, R. Gerhard-Multhaupt, in *2005 12th Inter. Symp. on Electrets*, IEEE, Piscataway, NJ, September **2005**, pp. 47–50.
- [86] A. M. Savijarvi, M. Paajanen, E. Saarimaki, H. Minkkinen, in *2005 12th Inter. Symp. on Electrets*, IEEE, Piscataway, NJ, September **2005**, pp. 75–78.
- [87] Y. Li, C. Zeng, *Macromol. Chem. Phys.* **2013**, *214*, 2733.
- [88] D. P. Erhard, D. Lovera, W. Jenninger, J. Wagner, V. Altstadt, H. W. Schmidt, *Macromol. Chem. Phys.* **2010**, *211*, 1719.
- [89] N. Behrendt, *IEEE Trans. Dielectr. Electr. Insul.* **2010**, *17*, 1113.
- [90] X. Qiu, L. Holländer, R. F. Suárez, W. Wirges, R. Gerhard, *Appl. Phys. Lett.* **2010**, *97*, 072905.
- [91] M. Sborikas, X. Qiu, W. Wirges, R. Gerhard, W. Jenninger, D. Lovera, *Appl. Phys. A* **2014**, *114*, 515.
- [92] W. R. McCall, K. Kim, C. Heath, G. La Pierre, D. J. Sirbuly, *ACS Appl. Mater. Interfaces* **2014**, *6*, 19504.
- [93] A. Kachroudi, S. Basrou, L. Rufer, A. Sylvestre, F. Jomni, *Smart Mater. Struct.* **2016**, *25*, 105027.
- [94] S. Cha, S. M. Kim, H. Kim, J. Ku, J. I. Sohn, Y. J. Park, B. G. Song, M. H. Jung, E. K. Lee, B. L. Choi, J. J. Park, Z. L. Wang, J. M. Kim, K. Kim, *Nano Lett.* **2011**, *11*, 5142.
- [95] N. Jahan, F. Mighri, D. Rodrigue, A. Ajji, *J. Appl. Polym. Sci.* **2019**, *136*, 47540.
- [96] S. Zhukov, X. Ma, H. V. Seggern, G. M. Sessler, O. B. Dali, M. Kupnik, X. Zhang, *Appl. Phys. Lett.* **2020**, *117*, 112901.
- [97] N. Behrendt, V. Altstadt, H. W. Schmidt, X. Zhang, G. M. Sessler, *IEEE Trans. Dielectr. Electr. Insul.* **2006**, *13*, 992.
- [98] H. Gilbert-Tremblay, F. Mighri, D. Rodrigue, *J. Cell. Plast.* **2012**, *48*, 341.
- [99] E. Klimiec, B. Królikowski, M. Machnik, W. Zaraska, J. Dzwonkowski, *J. Electron. Mater.* **2015**, *44*, 2283.
- [100] H. Kaczmarek, B. Królikowski, E. Klimiec, J. Kowalonek, *J. Mater. Sci.: Mater. Electron.* **2017**, *28*, 6435.
- [101] H. Kaczmarek, M. Chylińska, B. Królikowski, E. Klimiec, D. Bajer, J. Kowalonek, *J. Mater. Sci.: Mater. Electron.* **2019**, *30*, 21032.
- [102] H. Kaczmarek, B. Królikowski, M. Chylińska, E. Klimiec, D. Bajer, *Polymers* **2019**, *11*, 1345.
- [103] S. K. Ghosh, T. K. Sinha, B. Mahanty, D. Mandal, *Energy Technol.* **2015**, *3*, 1190.
- [104] S. K. Ghosh, A. Biswas, S. Sen, C. Das, K. Henkel, D. Schmeisser, D. Mandal, *Nano Energy* **2016**, *30*, 621.
- [105] B. Mahanty, S. K. Ghosh, S. Garain, D. Mandal, *Mater. Chem. Phys.* **2017**, *186*, 327.
- [106] M. Rahimabady, E. C. Statharas, K. Yao, M. Sharifzadeh Mirshekarloo, S. Chen, F. E. H. Tay, *Appl. Phys. Lett.* **2017**, *111*, 241601.
- [107] N. Jahan, F. Mighri, D. Rodrigue, A. Ajji, *J. Appl. Polym. Sci.* **2019**, *136*, 47929.
- [108] D. Xu, H. Zhang, L. Pu, L. Li, *Compos. Sci. Technol.* **2020**, *192*, 108108.
- [109] M. A. Ansari, P. Somdee, K. Marossy, *J. Polym. Res.* **2021**, *28*, 1.
- [110] C. A. Petroff, T. F. Bina, G. R. Hutchison, *ACS Appl. Energy Mater.* **2019**, *2*, 6484.
- [111] C. Xu, L. Jin, L. Zhang, C. Wang, X. Huang, X. He, Y. Xu, R. Huang, C. Zhang, W. Yang, J. Lu, *Compos. Sci. Technol.* **2018**, *164*, 282.
- [112] C. Baur, D. J. Apo, D. Maurya, S. Priya, W. Voit, *Polymer Composites For Energy Harvesting, Conversion, and Storage*, American Chemical Society, Washington, DC **2014**, pp. 1–27.
- [113] D. Shen, Doctoral Dissertation, ProQuest LLC, United States **2009**.
- [114] F. Seidi, C. Deng, Y. Zhong, Y. Liu, Y. Huang, C. Li, H. Xiao, *Small* **2021**, *17*, 2102453.
- [115] P. Abdollahiyan, M. Hasanzadeh, P. Pashazadeh-Panahi, F. Seidi, *J. Mol. Liq.* **2021**, *338*, 117020.
- [116] F. Seidi, M. Reza Saeb, Y. Huang, A. Akbari, H. Xiao, *Chem. Rec.* **2021**, *21*, 1876.
- [117] A. Saadati, M. Hasanzadeh, F. Seidi, *TrAC, Trends Anal. Chem.* **2021**, *142*, 116308.
- [118] H. Kholafazad-Kordasht, M. Hasanzadeh, F. Seidi, *TrAC, Trends Anal. Chem.* **2021**, *145*, 116455.
- [119] F. Seidi, A. Arabi Shamsabadi, A. Ebadi Amooghini, M. R. Saeb, H. Xiao, Y. Jin, M. Rezakazemi, *Environ. Chem. Lett.* **2022**, *20*, 1083.
- [120] Z. Shokri, F. Seidi, M. R. Saeb, Y. Jin, C. Li, H. Xiao, *Mater. Today Chem.* **2022**, *24*, 100780.
- [121] F. Seidi, M. R. Saeb, Y. Jin, P. Zinck, H. Xiao, *Mini-Rev. Org. Chem.* **2022**, *19*, 416.
- [122] S. Sardarelli, M. Hasanzadeh, F. Seidi, *J. Mol. Recognit.* **2021**, *34*, e2928.
- [123] F. Seidi, D. Crespy, *Chem. Commun.* **2020**, *56*, 11931.
- [124] F. Seidi, W. Zhao, H. Xiao, Y. Jin, M. R. Saeb, C. Zhao, *Polym. Chem.* **2020**, *11*, 4355.
- [125] A. Saadati, M. Ehsani, M. Hasanzadeh, F. Seidi, N. Shadjou, *Microchem. J.* **2021**, *169*, 106610.
- [126] C. H. Sun, G. Q. Shang, Y. Y. Tao, Z. R. Li, *Adv. Mater. Res.* **2012**, *516*, 1481.
- [127] F. Farshchi, A. Saadati, H. Kholafazad-Kordasht, F. Seidi, M. Hasanzadeh, *J. Mol. Recognit.* **2021**, *34*, e2927.
- [128] S. Karimi, F. Seidi, M. Niakan, H. Shekaari, M. Masteri-Farahani, *Renewable Energy* **2021**, *180*, 132.
- [129] F. Seidi, Y. Jin, H. Xiao, *Carbohydr. Polym.* **2020**, *242*, 116277.
- [130] F. Seidi, W. Zhao, H. Xiao, Y. Jin, C. Zhao, *Chem. Rec.* **2020**, *20*, 857.
- [131] H. K. Kordasht, M. Hasanzadeh, F. Seidi, P. M. Alizadeh, *TrAC, Trends Anal. Chem.* **2021**, *140*, 116279.
- [132] A. Mobed, M. Hasanzadeh, F. Seidi, *RSC Adv.* **2021**, *11*, 34688.
- [133] H. Nosrati, F. Seidi, A. Hosseinmirzaei, N. Mousazadeh, A. Mohammadi, M. Ghaffarloo, H. Danafar, J. Conde, A. Sharafi, *Adv. Healthcare Mater.* **2022**, *11*, 2102321.
- [134] E. D. Aminabad, A. Mobed, M. Hasanzadeh, M. A. H. Feizi, R. Safaralizadeh, F. Seidi, *RSC Adv.* **2022**, *12*, 4346.
- [135] S. Crossley, R. A. Whiter, S. Kar-Narayan, *Mater. Sci. Technol.* **2014**, *30*, 1613.
- [136] H. Li, Z. D. Deng, T. J. Carlson, *Sensor Lett.* **2012**, *10*, 679.
- [137] T. H. Kim, M.Sc. Thesis, >University of California at Berkeley **2015**.
- [138] R. Kour, A. Charif, *Innov. Energy Res.* **2016**, *5*.
- [139] G. W. Taylor, J. R. Burns, S. A. Kammann, W. B. Powers, T. R. Welsh, *IEEE J. Oceanic Eng.* **2001**, *26*, 539.
- [140] S. Priya, C. T. Chen, D. Fye, J. Zahnd, *Jpn. J. Appl. Phys.* **2004**, *44*, L104.
- [141] M. A. Karami, J. R. Farmer, D. J. Inman, *Renewable Energy* **2013**, *50*, 977.
- [142] F. Qian, M. Liu, J. Huang, J. Zhang, H. Jung, Z. D. Deng, M. R. Hajj, L. Zuo, *Renewable Energy* **2022**, *187*, 34.

- [143] E. E. Aktakka, H. Kim, K. Najafi, *J. Micromech. Microeng.* **2011**, 21, 095016.
- [144] M. Safaei, R. I. Ponder, S. R. Anton, *Active and Passive Smart Structures and Integrated Systems XII*, Denver, Colorado, United States Vol. 10595, International Society for Optics and Photonics **2018**, p. 105951Q.
- [145] H. Zhang, X. S. Zhang, X. Cheng, Y. Liu, M. Han, X. Xue, S. Wang, F. Yang, S. A S, H. Zhang, Z. Xu, *Nano Energy* **2015**, 12, 296.
- [146] J. Zhao, Z. You, *Sensors* **2014**, 14, 12497.
- [147] M. Pozzi, M. S. Aung, M. Zhu, R. K. Jones, J. Y. Goulermas, *Smart Mater. Struct.* **2012**, 21, 075023.
- [148] S. J. Hwang, H. J. Jung, J. H. Kim, J. H. Ahn, D. Song, Y. Song, H. L. Lee, S. P. Moon, H. Park, T. H. Sung, *Curr. Appl Phys.* **2015**, 15, 669.
- [149] I. Jung, Y. H. Shin, S. Kim, J. Y. Choi, C. Y. Kang, *Appl. Energy* **2017**, 197, 222.
- [150] S. R. Anton, S. G. Taylor, E. Y. Raby, K. M. Farinholt, *Industrial and Commercial Applications of Smart Structures Technologies 2013*, Vol. 8690, International Society for Optics and Photonics, San Diego, California, United States March, **2013**, p. 869007.
- [151] M. H. Malakooti, B. A. Patterson, H. S. Hwang, H. A. Sodano, *Energy Environ. Sci.* **2016**, 9, 634.
- [152] X. Xie, Q. Wang, *Int. J. Eng. Sci.* **2015**, 94, 113.
- [153] K. B. Singh, V. Bedekar, S. Taheri, S. Priya, *Mechatronics* **2012**, 22, 970.
- [154] M. A. Ansari, N. Jahan, *Mater. Highlights* **2021**, 2, 23.
- [155] M. A. Ansari, *Appl. Phys. A* **2021**, 127, 1.
- [156] S. Bhalla, S. Moharana, V. Talakokula, N. Kaur, *Piezoelectric Materials: Applications in SHM, Energy Harvesting and Biomechanics*, John Wiley & Sons, Chichester, UK **2016**.
- [157] V. Pratibha Arun, D. Mehta, *Int. J. Eng. Res. Appl.* **2013**, 3, 478.



**Manauwar Ali Ansari** received his M.Sc. in materials engineering from the Institute of Ceramics and Polymer Engineering, University of Miskolc, Miskolc, Hungary, in 2020. He is currently doing his doctoral research at Hevesy György PhD School of Chemistry, ELTE, Hungary. His interests and expertise are in the fields of energy and functional materials, synthesis and characterization of nanomaterials, polymers, interfacial phenomenon, quantum materials, nanothermodynamics, and superconductivity.



**Patcharapon Somdee** received her M.Eng. from the Suranaree University of Technology, Thailand, in 2009. She obtained her Ph.D. from the University of Miskolc, Hungary, and is currently a lecturer at the Rajamangala University of Technology Isan, Thailand. Her research interests are in thermally conductive polymer, polymer blends, polymer composites, and biodegradable plastics.